Diversity metrics of pelagic archaeal and bacterial communities in San Francisco Bay depend on scale

Anna Rasmussen[1], Julian Damashek[1†], Emiley Eloe-Fadrosh[2], and Christopher A. Francis[1*]

[1]Department of Earth System Science, Stanford University, Stanford, CA 94305, USA

[2]Department of Energy Joint Genome Institute, Walnut Creek, California 94598, USA

*Correspondence: Christopher Francis, Department of Earth System Science, 473 Via Ortega, Y2E2 Bldg Rm 140, Stanford University, Stanford, CA 94305, USA. Email: caf@stanford.edu

Running Title: Pelagic bacteria and archaea of San Francisco Bay

[†]Present Address: Department of Biology, Utica College, Utica, NY 13502, USA

Originality-Significance Statement

This is the first assessment of the biogeography of pelagic bacteria and archaea in San Francisco Bay using high throughput sequencing. We amplified the V4 and V4-V5 regions of the 16S rRNA gene in 174 samples collected during a two-year monthly time series along a 150-km transect of San Francisco Bay using two different 'universal' primer pairs. We analyze diversity metrics at several taxonomic levels and different physicochemical extents to reveal patterns in richness, nestedness, turnover, and site-specificity and gain further insight into estuarine microbial community structure. At the 97% OTU level, site-specificity and turnover are high while at the phylum level organisms are more broadly distributed and the community is more nested.

SUMMARY

This study uses high throughput sequencing (HTS) to examine bacterioplankton and archaeoplankton communities in 174 samples collected along a 150-km transect in San Francisco Bay over a two-year monthly time-series. To better understand microbial biogeography in San Francisco Bay, we analyzed communities using two different sets of 16S rRNA primer sets at several taxonomic levels to reveal patterns in richness, nestedness, and site-specificity. Our analysis reveals that both updated V4 and V4-V5 primers similarly describe diverse estuarine microbial communities. We find that OTUs (97% identity) show high site-specificity, occurring in a small subset of samples either defined by narrow salinity or temporal ranges. At the OTU level, turnover is high along the salinity gradient and distinct brackish communities are observed. At coarser taxonomic levels (e.g. phylum, class) taxa are broadly distributed across salinity zones and communities appear to be a mix of fresh and marine end-member communities. However, differential abundance testing shows that, despite high prevalence across salinity zones, most phyla have preferences for a narrower salinity range. While salinity is the dominant force shaping community structure, seasonal variations in communities are observed within salinity zones. In addition, suspended particulate matter concentrations are linked to patterns in alpha and beta diversity.

INTRODUCTION

San Francisco Bay (SFB) is the largest estuary on the west coast of the continental United States and is surrounded by approximately 7.6 million people (US Census Bureau 2017). SFB consists of two arms, generally referred to as North and South Bay, which have differing freshwater sources and water residence times (Walters *et al.*, 1985; Kimmerer, 2004). North Bay is river-dominated and includes San Pablo bay, Suisun bay, and the Delta region while South Bay is a weakly mixed marine lagoon. Intense urban development along the shores and other human activities such as damming, diking, dredging, historic mining, and pollution have led SFB to be considered one of the most anthropogenically altered estuaries in the United States (Nichols *et al.*, 1986).

Long term monitoring projects from both federal and state agencies have also made SFB one of the most studied estuaries in the world (Kimmerer, 2004) and, consequently, SFB has served as a model for understanding physical, chemical, and biological estuarine dynamics (Cloern, 1996, 2001; Lucas *et al.*, 1998, 2009; Cloern and Jassby, 2012; Raimonet and Cloern, 2017). For over four decades, water quality in SFB has been monitored regularly by the United States Geological Survey (USGS) (Schraga and Cloern, 2017), showing both gradual and abrupt changes in water quality due to human activity (Cloern *et al.*, 2017; Beck *et al.*, 2018; Cloern, 2019) and leading to a thorough characterization of phytoplankton dynamics (Cloern, 1987; Cloern and Dufford, 2005; Cloern and Jassby, 2010; Sutula *et al.*, 2017). In contrast to the in-depth monitoring of phytoplankton in SFB, bacterioplankton and archaeoplankton populations are remarkably understudied in this system. In fact, only three studies to date have examined pelagic microbial

community structure in SFB (Murray *et al.*, 1996; Hollibaugh *et al.*, 2000; Stepanauskas *et al.*, 2003), all of which used molecular approaches with limited phylogenetic resolution (i.e. DGGE, T-RFLP) or sequencing depth. Here, we build considerably on this literature, using deep 16S rRNA amplicon sequencing at a large spatial and temporal scale to understand bacterial and archaeal ecology in the turbid estuarine waters of SFB.

SFB is an excellent model system for understanding microbial community dynamics because it encompasses both spatial (e.g. salinity) and temporal (e.g. temperature) physicochemical gradients (Cloern *et al.*, 2017). Salinity has been identified as a universal driver of prokaryotic community structure (Lozupone and Knight, 2007; Thompson *et al.*, 2017), as well as a key driver of estuarine bacterial community composition in numerous studies (Crump *et al.*, 1999, 1999, 2004, 1999; Fortunato and Crump, 2011; Herlemann *et al.*, 2011; Fortunato *et al.*, 2012; Mason *et al.*, 2016; Doherty *et al.*, 2017). However, studies in estuarine environments have also identified drivers of microbial community structure besides salinity, including temperature, pH, dissolved oxygen, water residence time, organic carbon or nutrient availability (Murrell *et al.*, 1999; Hollibaugh *et al.*, 2000; Crump *et al.*, 2004; Herlemann *et al.*, 2011; Liu *et al.*, 2014; Satinsky *et al.*, 2014). To further assess broader scale patterns in microbial biogeography, we investigate diversity metrics at varying taxonomic grain sizes (Thompson *et al.*, 2017; Ladau and Eloe-Fadrosh, 2019).

While we expect salinity to be the main driver of community structure in SFB, we address the following questions: What other environmental variables influence alpha and beta diversity

metrics throughout the bay and within different salinity zones? Are samples nested along the salinity gradient? How does taxonomic grain size impact diversity metrics? Do most organisms have broad or narrow distributions? How does primer choice impact the characterization of microbial community composition and structure? We sampled 12 stations ranging from fresh riverine inputs to brackish mixing zones to highly marine-influenced regions along a ~150-km transect of the SFB channel. We sequenced bottom water samples collected monthly over two-years, capturing microbial communities across several seasonal gradients (e.g. temperature, freshwater flow rate) as well. Amplicon libraries were generated using two updated 16S rRNA primer sets, which amplify variable region 4 (Apprill *et al.*, 2015; Parada *et al.*, 2016) and regions 4 and 5 (Parada *et al.*, 2016), respectively. Both primer sets were designed to remedy known biases against SAR11 and Thaumarchaeota—two of the most abundant microbial taxa on Earth and important organisms in marine and estuarine environments, including San Francisco Bay.

RESULTS & DISCUSSION

Environmental Data. Water column samples within this dataset correspond to salinities ranging from fresh (minimum 0.07) to euhaline (maximum 32.42) and temperatures from 6.8 to 22.7 °C (Fig.1). Examples of stations typically falling into the Venice salinity zones (Battaglia, 1959) are as follows: station 657 is fresh (<0.5), 649 is oligohaline (.05 to <5), 6 is mesohaline (5 to <18), 13 is polyhaline (18 to <30), and 18 is euhaline (30 to <40) (Fig. 1). Chlorophyll a concentrations were typically low (~3µg/L) with peaks concentrations occurring in late winter/spring and in South Bay (Fig. S1). Ammonium concentrations were highest in riverine samples due to inputs

from the Sacramento Regional WWTP, while nitrate concentrations were highest in Lower South Bay (Fig. S1). Nitrite concentrations occasionally reached high concentrations (>9 µM) in South Bay. High nitrite concentrations in this region of the bay have been reported previously (Wankel *et al.*, 2006; Damashek *et al.*, 2016). The wet season generally has lower temperatures, higher suspended particulate matter (SPM) concentrations, higher delta outflow, and lower salinities in each region of SFB when compared to the dry season (Fig S2).

Updated 16S rRNA V4 and V4-V5 primers similarly describe estuarine microbial communities. For the remainder of this text, 16S rRNA libraries amplified by the 515F-Y (Parada *et al.*, 2016) and 806RB (Apprill *et al.*, 2015) primers will be referred to as the 'V4 dataset' and libraries amplified by 515F-Y and 926R (Parada *et al.*, 2016) will be referred to as the 'V4-V5' dataset, based on which variable regions they amplify. While library sizes vary between sequencing runs and primer pairs, the general description of microbial communities is strikingly similar. Despite some differences in taxonomy between datasets (Table S1), large-scale interpretation of alpha and beta diversity is essentially the same for both primer pairs (Fig. S3). The relative abundance of phyla that occur in both primer sets is strongly correlated (Fig. S3A; $r^2 = 0.99$, $p < 0.001$), as is the richness within phyla (Fig. S3B; $r^2 = 0.99$, $p < 0.001$). There is also a correlation between the relative abundance of top genera (Fig. S3C; $r^2 = 0.74$, $p < 0.0001$). Sample richness is correlated between primer pairs ($r^2 = 0.83$, $p < 0.001$) and mostly strongly correlated to SPM for both primer pairs (Table S2). Procrustes analyses of PCoA ordinations reveal very similar patterns (Fig. S3D; $m^2 = 0.007$, $r^2 = 0.996$) and relationships between PCoA axes and environmental variables are also consistent (Table S2).

Since updated primers were paired and tested with mock communities lacking both SAR11 and *Thaumarchaeota* (Walters *et al.*, 2016) and the updated V4 primer pair has subsequently been adopted by the Earth Microbiome Project (EMP), we are particularly interested in comparing diversity metrics of these environmentally-relevant groups. In this study, SAR11 and *Thaumarchaeota* are abundant in amplicon libraries constructed with both primer pairs, and display similar distribution patterns (Fig. S4-S5).

While communities are generally similar in both datasets, there were some minor differences. We note that the V4-V5 dataset contains more phyla but fewer OTUs (Table S1) and there are differences in the relative abundances of certain groups of organisms (Fig. S3A,C). For example, some archaea are more relatively abundant in the V4-V5 dataset (*Thaumarchaeota* and *Bathyarchaeota*) while others are more relatively abundant in the V4 (*Woesarchaeota and Euryarchaeota*) (Fig. S6). Despite these differences in relative abundance, beta diversity metrics are very similar for each dataset including the whole community (Fig. S3D) or just archaeal OTUs (Fig. S6). Thus, depending on the target organisms or analyses of interest, one primer pair may be better than the other, but for overall community diversity analysis of estuarine samples both primer pairs work similarly. Most diversity metrics are similar regardless of primer pair (Fig. S3, Table S2) and differences occurring in classification of OTUs could in part be due to differing amplicon lengths.

Salinity, SPM, seasonality, and region influence community structure in SFB. We used a variety of analyses to assess beta diversity. We expected salinity to be a key factor in shaping communities, as observed in a wide variety of estuaries (Crump *et al.*, 2004; Hewson and Fuhrman, 2004; Herlemann *et al.*, 2011; Fortunato *et al.*, 2012; Aguirre *et al.*, 2017), and the findings in our study agree with this body of literature. First we used ordination analyses to assess beta diversity based on Bray-Curtis dissimilarity between communities. The first two axes explain 54.3% of total variation in PCoA plots (Fig. 2). Salinity is strongly correlated to Axis 1 in PCoA plots ($r^2 = 0.94$, $p < 0.001$; Table S2). Based on a "goodness of clusters" gap statistic, PCoA ordination forms 4 clusters that generally correspond with salinity zone [fresh (<0.5), oligohaline (.05 to <5), mesohaline (5 to <18), polyhaline (18 to <30), and euhaline (30 to <40)], with polyhaline and euhaline samples forming less distinct groupings (Fig. S7). Using the *betapart* function, we confirm that turnover is a much larger component than nestedness in community dissimilarity metrics (Table S3). A heatmap based on Bray-Curtis dissimilarity and hierarchical clustering based on Jaccard dissimilarity both show that samples generally group by salinity zone (Fig. S8). Graph-based testing using Friedman-Rafsky tests on a minimum spanning tree, a distance-threshold graph, and a k-nearest neighbor graph all show that samples within salinity zones contain more pure edges than the null distribution ($p < 0.001$, Fig. S9), indicating samples within a salinity zone are more similar to one another than expected by chance. Taken together, ordination, hierarchical clustering, and graph-based tests all support that salinity zone definitions are ecologically relevant.

Spatial/salinity gradients have overwhelmed seasonal variation in other estuarine communities (Fortunato *et al.*, 2012) so we examined diversity metrics within salinity zones. PCoA ordinations within a given salinity zone reveal stronger seasonal groupings. In fresh, oligohaline, and mesohaline ordination plots, there is a separation between samples from the wet versus the dry season (Fig. S10). Axes correlate strongly with variables that vary seasonally, including temperature and SPM (Table S4).

Inspection of ordinations, networks, and heatmaps shows that polyhaline and euhaline samples may cluster together more than other zones (Figs. 2, S7-S9), but also indicates that South and North Bay samples are more distinct from one another even when samples have similar salinities. This may be unsurprising given the differences in residence times and hydrology in the two arms of the bay (Walters *et al.*, 1985; Kimmerer, 2004), leading them to often be classified as two separate ecosystems. We investigated South Bay and North Bay samples separately. While beta diversity in the North Bay is predominantly influenced by salinity, ordinations of South Bay samples show a strong influence of SPM and temperature on axes 1 and 2, respectively (Fig. 2, Table S4).

SPM concentration influences both alpha diversity measures of richness (Fig. 3) and beta diversity (Fig. 2) of pelagic bacteria and archaea in SFB. Community richness most strongly correlates with SPM concentrations at all taxonomic levels (i.e. phylum through OTU) and does not appear to strongly correspond to salinity (Table S2). Richness of samples within each salinity zone and in either North or South Bay is most strongly correlated to SPM (Fig. S10, Table S4).

193 SPM varies over space and time, which can make other spatial and temporal patterns in
194 richness difficult to observe (Fig. 3). In PCoA ordinations of all SFB samples, axis 2 most strongly
195 correlates to SPM (Fig. 2, Table S2). NODF-based nestedness analyses support that less-
196 rich/low-SPM communities are a nested subset of richer, high-SPM associated communities at
197 the phylum through genus level but not the OTU level (Fig. 4). Thus, at the finest taxonomic
198 scale (OTU 97%), less-rich/low-SPM communities do not appear to be a nested subset of more-
199 rich/high-SPM communities (Fig. 4). Our findings that communities are nested at coarser
200 taxonomic levels is in agreement with a previous study that found free-living and particle-
201 associated communities were very similar using DGGE (Hollibaugh *et al.*, 2000), a technique
202 that may have identified organisms at a coarser taxonomic scale than the 97% identity OTU
203 level.
204
205 SPM could be important for microbial community composition because it provides nutrients for
206 organisms and/or has a long residence time that allows unique, particle-associated
207 communities to form on and around particles (Hollibaugh *et al.*, 2000). Indeed, phytoplankton
208 dynamics and bacterioplankton activity have been linked to SPM dynamics in SFB (Cloern, 1987;
209 Hollibaugh and Wong, 1999; Murrell *et al.*, 1999; Hollibaugh *et al.*, 2000, 200). Microbes
210 associated with resuspended sediments could also explain the potential distinction between
211 low- and high-SPM associated communities. This idea is supported by the negative correlation
212 between richness and the ratio of active chlorophyll *a* to degraded phaeopigments (Table S2). A
213 low ratio of active chlorophyll *a* to phaeopigments indicates strong resuspension of bottom
214 sediments, which are rich in degraded algal material. Our study does not differentiate between

215 'free-living' and 'particle-associated' organisms using the same size fractions as in Hollibaugh *et*
216 *al.* (2000) and includes all organisms small enough to pass through a 10 µm filter but captured
217 by a 0.22 µm filter. While our findings indicate that particle-associated communities could be
218 more diverse and distinct from free-living communities, further studies are necessary to directly
219 address differences between various size fractions of particle-associated versus free-living
220 communities at the OTU level as well as tease apart the relationships between microbial
221 community composition and SPM quantity, quality, and source.
222
223 **Salinity tolerance varies at different taxonomic grain sizes.** To further understand how
224 communities change along the salinity gradient, we looked more deeply at community diversity
225 nestedness and taxa entropy. We used the NODF statistic to calculate if less rich communities
226 were a subset of richer communities. We find that communities are highly nested at coarser
227 taxonomic levels (e.g. phylum, class) and become gradually less nested at finer taxonomic
228 levels, before becoming substantially less nested at the OTU level (Fig. 4). All NODF statistics are
229 significantly greater than the null model values except at the OTU level, indicating that at most
230 taxonomic scales less diverse communities are to some extent a nested subset of more diverse
231 communities (Fig. 4). The lack of significance and low NODF values indicate that OTUs are not
232 nested.
233
234 We also calculated entropy using the Shannon index as a measure of site-specificity (i.e. how
235 many different samples a given taxa occurs in) of a given taxa. Entropy of taxa decreases from
236 coarse to finer taxonomic scales (Fig. 4), indicating that the site-specificity of taxa increases at

237 finer scales such as at the OTU level. Higher entropy values at the phylum level indicate less
238 site-specificity, while lower entropy values at the OTU level indicate greater site-specificity. This
239 can also be observed visually in relative abundance bar plots, with most abundant phyla
240 occurring across a broad range of samples while abundant genera or OTUs occur in a smaller
241 subset of samples (Fig. 5, Fig. S11-S16).
242
243 Nestedness and taxa entropy are both greater at coarse taxonomic levels and gradually
244 decrease from the phylum to genus level, then decrease substantially at the OTU level (Fig. 4).
245 These findings support that at the phylum level, organisms have broader salinity tolerance but
246 organisms at the 97% identity level are adapted to a specific salinity range and turnover is high
247 along the salinity gradient, potentially with closely related organisms replacing their more or
248 less salt-tolerant relatives along the gradient. Bar plots reveal clear patterns in each salinity
249 zone, with a gradual distinction between freshwater and saline sites at the class and order level,
250 followed by more specific mesohaline communities emerging at the genus and OTU level (Figs.
251 S11-16). Because richness is not correlated strongly with salinity at any taxonomic level,
252 communities are not necessarily nested along the salinity gradient. Rather, the low nestedness
253 of OTUs and partitioning of beta diversity metrics indicate that turnover dominates along the
254 salinity gradient (Fig. 2, Fig. 4, Table S3). The high nestedness of samples at the phylum level
255 and low nestedness at the OTU level agrees with recent findings from the EMP dataset
256 (Thompson *et al.*, 2017) and support similar findings in the brackish Baltic Sea (Herlemann *et*
257 *al.*, 2011). Interestingly, differential abundance testing shows most phyla (33/46) vary
258 significantly in abundance across salinity zones (Fig. 4, S17). At all taxonomic levels, many taxa

(between 40 and 75%) show significant variation in abundance between the five salinity zones (Fig. 4). OTUs show the greatest magnitude of abundance change (Fig. 4). Thus, while phyla have broader distributions along the salinity gradient in terms of presence/absence there are significant variations in abundance between salinity zones, supporting that even at the phylum level there are ecologically meaningful adaptations based on salinity.

Abundant microbial taxa in SFB

The top 10 phyla in the V4 and V4-V5 datasets are *Proteobacteria*, *Bacteroidetes*, *Actinobacteria*, *Verrucomicrobia*, *Cyanobacteria*, *Thaumarchaeota*, *Planctomycetes*, *Euryarchaeota*, *Marinimicrobia*, and *Acidobacteria* (Fig. S11). OTUs in these 10 phyla account for over 90% of reads in each sample (Fig. S11). These abundant phyla have broad distributions across samples, though differential abundance testing shows that only *Bacteroidetes*, *Thaumarchaeota*, and *Cyanobacteria* do not have significant changes in abundance between salinity zones (Figs. S17). Of these abundant phyla, *Actinobacteria*, *Verrucomicrobia*, and *Acidobacteria* are more abundant near fresh end-member sites while *Marinimicrobia*, *Euryarchaeota*, *Planctomycetes*, and *Proteobacteria* are more abundant closer to marine end-member sites.

Proteobacteria is the most abundant and richest phylum in the SFB dataset (Fig. S2). Common patterns observed in estuaries such as decreasing *Betaproteobacteria* and increasing *Alpha-* and *Gammaproteobacteria* with increasing salinity (Murray *et al.*, 1996; Crump *et al.*, 1999, 1999; Bouvier and Giorgio, 2002; Zhang *et al.*, 2006; Kan *et al.*, 2008; Herlemann *et al.*, 2011)

were also observed in our study (Fig. S11,). At the order level, *Oceanospiralles* and *Rhodobacterales* are more abundant in marine-influenced samples and *Burkholderales* dominates in freshwater end-member stations (S13). In general, OTUs have lower entropy (higher site-specificity) and abundant OTUs have narrower salinity ranges than observed at coarser taxonomic levels within the *Proteobacteria* (e.g. class, order, family) (Fig. S11). Richness of *Proteobaceteria* OTUs is most strongly correlated with SPM concentrations (r^2 = 0.42) and ordinations highlight the prominent role of salinity in shaping the *Proteobacteria* community (Fig. S11).

Unlike other orders of *Proteobacteria*, SAR11 clade bacteria (*Alphaproteobacteria*) are abundant along the entire salinity gradient. SAR11 are the most abundant organisms at the order level (generally ~10-30% of reads in a sample), constitute one of the most abundant genera (*Pelagibacter*), and correspond to many of the top OTUs in our dataset (Figs. 5, S5, S11). SAR11 are highly structured along the salinity gradient in SFB, a pattern observed in other estuaries (Kan *et al.*, 2008; Campbell and Kirchman, 2013; Herlemann *et al.*, 2014). The abundance of SAR11 in our dataset bolsters previous findings in SFB indicating that SAR11 clade bacteria are ubiquitous (Murray *et al.*, 1996) and LD12 organisms are abundant in fresh sites (Stepanauskas *et al.*, 2003). The distribution of 'LD12 clade' organisms in our study aligns with findings from recent cultured isolates (Henson *et al.*, 2018), with peak LD12 abundances occurring in primarily fresh and oligohaline sites (salinity < 5; Fig. S11). LD12 are proposed to be specialized to freshwater environments through the loss of key compatible solute genes (Henson *et al.*, 2018), highlighting one way this group may have differentiated itself from its

303 relatives and adapted to a specific niche. A family identified as the 'Chesapeake Delaware Bay
304 clade' [SAR11 IIIa (Kan *et al.*, 2008)] is most abundant at mesohaline and oligohaline sites, while
305 'Surface 1' [SAR11 Ia (Vergin *et al.*, 2013)] OTUs dominate at poly- and euhaline sites. This
306 partitioning of groups along the salinity gradient can also be observed from the family to the
307 OTU level (Figs. 5 & S5). Seasonal variations in SAR11 communities are also observed in
308 ordination plots (Figs. S5).
309
310 *Bacteroidetes*, and particularly *Flavobacteriia*, which are important for the breakdown of
311 organic matter in estuaries and coasts (Williams *et al.*, 2013; Smith *et al.*, 2017, 201), are also
312 abundant in SFB waters (Fig. S11). *Bacteroidetes* is the second most abundant and second
313 richest phylum in the dataset (Fig. S3), in agreement with previous findings that marine
314 *Flavobacteria* have high global and local diversity (Alonso *et al.*, 2007). *Flavobacteriales* is one
315 of the most abundant orders in the dataset. The NS5 marine clade genus of *Flavobacteriaceae*
316 is among the top genera (Figs. S3 & S11). In fresh end-member stations the families
317 *Chitinophagaceae*, *Cytophagaceae*, and 'NS11-12 marine group' (Alonso *et al.*, 2007) dominate
318 (Fig. S14). Brackish stations are dominated by the family *Cryomorphaceae* while marine end-
319 member stations are dominated by *Flavobacteraceae*. Bacteroidetes OTUs are more site-
320 specific and have narrower salinity tolerance than at coarser taxonomic levels and richness is
321 most strongly correlated to SPM concentrations (Fig. S14, $r^2 = 0.49$).
322
323 *Actinobacteria* is the third most abundant phylum in SFB. *Candidatus Actinomarina* and 'hgcI
324 clade' (Glöckner *et al.*, 2000) are among the top genera (Figs. S3 & S11), with diverse 'hgcI

clade' organisms dominating freshwater end member stations and *Ca. Actinomarina*-like OTUs dominating in more saline samples (Fig. S12 & S15). Other estuarine studies have found high diversity and specialization of *Actinobacteria* with differing environmental gradients (Kirchman *et al.*, 2005; Holmfeldt *et al.*, 2009; Campbell and Kirchman, 2013), which we observe as well. *Actinobacteria* richness is most strongly correlated with salinity and ordination plots show strong separation of communities based on wet versus dry season (Fig. S15). While there appears to be more OTU-level diversity in the freshwater stations, only one *Ca. Actinomarina-like* OTU (OTU 0) dominates the most marine-influenced station (18). Poly/Euhaline stations 13 and 27 are dominated by OTUs 0 and 8, indicating microdiversity may exist below the 97% OTU definition (Fig S12 & S16). Metagenomes of *Ca. Actinomarina* organisms suggest they are very small, free-living photoheterotrophic organisms co-occuring with *Synechococcus* in marine photic zones and containing streamlined and low-GC genomes with novel rhodopsins (Ghai *et al.*, 2013; Mizuno *et al.*, 2015). *Ca. Actinomarina*-like OTU 8 can reach over 10% relative abundance in late summer in South Bay station 27 and shows smaller but noticeable peaks in station 13 as well (Fig. S12 & S16). Both fresh and marine planktonic *Actinobacteria* have been described as photoheterotrophs, and some are capable of degradation of recalcitrant organic matter (Ghai *et al.*, 2014), highlighting their potential functional role in SFB.

Cyanobacteria are generally low abundance in non-summer months in SFB and are dominated by *Synecchococcus*-like organisms (Fig. 5). Ordination plot shows strong seasonal variation in *Cyanobacteria* communities (Fig. S18). While salinity most strongly impacts community structure for most taxa, we do observe seasonal variation within groups such as *Cyanobacteria*,

347 *Actinobacteria*, and SAR11. Stronger temporal variations within specific taxonomic groups as
348 compared to the whole community have been observed in other estuaries (Fortunato *et al.*,
349 2013, 2; Li *et al.*, 2017).
350
351 Bacteria are relatively more abundant than archaea, which make up only ~2% of the overall
352 reads in our dataset. In freshwater sites, archaea generally have a low relative abundance (0.02
353 – 0.2%) and are predominantly *Woesearchaeota* and *Thaumarchaeota* (Fig. S6). However, in
354 poly- and euhaline sites *Thaumarchaeota* and *Euryarchaeota* can become abundant, comprising
355 over 20% and roughly 6% of reads, respectively (Fig. S6).
356
357 *Thaumarchaeota* genera and OTUs are distinct at the fresh and marine end-member sites, with
358 organisms generally considered fresh (*Nitrosoarchaeum*-like) (Blainey *et al.*, 2011; Mosier *et al.*,
359 2012) populating station 657 and marine (*Nitrosopelagicus*) (Santoro *et al.*, 2015) populating
360 station 18 (Fig. 5). The apparent 'bloom' of *Thaumarchaeota* in South Bay, with putative
361 *Nitrospumilus*-like sequences comprising as much as 25% of the total reads, has not been
362 previously described for this system. Blooms of *Thaumarchaeota* have been reported in other
363 estuaries in summer (Hollibaugh *et al.*, 2014; Schaefer and Hollibaugh, 2017), but also in coastal
364 areas in fall (Hu *et al.*, 2013; Kim *et al.*, 2019) or winter (Wuchter *et al.*, 2006; Pitcher *et al.*,
365 2011). Interestingly, this bloom is associated with nitrite accumulation (Fig. 5, $r^2 = 0.79$), a
366 phenomenon observed in other coastal and estuarine sites (Schaefer and Hollibaugh, 2017; Kim
367 *et al.*, 2019). Warmer temperatures between 20°C and 30°C have been proposed to explain the
368 decoupling of ammonia and nitrite oxidation in other systems; however, this SFB bloom occurs

in fall when temperatures are generally at or below 20°C and decreasing (Fig. 1). This apparent decoupling of ammonia and nitrite oxidation in South San Francisco Bay is intriguing and in need of further investigation. The high abundance of these *Thaumarchaeota* could also have implications for nitrogen cycling; indeed, nitrification rate measurements for this area of the bay are limited but could potentially be high (Damashek *et al.*, 2016).

Brackish communities are distinct at the OTU (97% similarity) level. While at the class and family level microbial communities appear to be a mix of freshwater and marine end-members (Figs. S11), at the OTU level communities display distinct fresh, brackish, and marine communities along the salinity gradient (Fig. S11-S16). Classes such as *Sphingobacteriia*, *Cytophagia*, *Actinobacteria*, and *Betaproteobacteria* are abundant at fresh end-member sites but decrease along the salinity gradient, as classes such as *Alphaproteobacteria*, *Gammaproteobacteria*, *Flavobacteriia*, and *Acidimicrobiia* become more abundant towards marine end-member sites (Fig. S11). At fresh and oligohaline sites, families such as *Comamonadaceae*, *Chitinophagaceae*, *Sporichthyaceae*, and 'LD freshwater clade' (SAR11) are abundant, while at polyhaline and euhaline sites *Rhodobacteraceae* and OM1 (*Actinobacteria*) are abundant (Fig. S11). At mesohaline sites, families such as 'Chesapeake Delaware Bay clade' [SAR11 IIIa (Kan *et al.*, 2008)] dominate. More distinct brackish communities start to emerge at the genus and OTU levels (Fig. S11). Some of the OTUs with highest abundance in brackish sites belong to taxa such as the SAR11 'Chesapeake Delaware Bay clade' (OTU 2), *Oceanospirillaceae* (OTU 13), *Hydrogenophilaceae* (OTU 55), *Ca. Actinomarina* (OTU 8), *Owenweeksia* (OTU 25), AEGEAN-169 clade of the *Rhodospirillaceae* family (OTU 14), and the NS5 marine group of the

391 *Flavobacteriaceae* family (OTU 13) (Figs. S12, S17). The uncultivated groups NS5 and AEGEAN-
392 169 have been associated with phytoplankton blooms or the breakdown of dissolved organic
393 matter (Gómez-Pereira *et al.*, 2010; Yang *et al.*, 2015; Bennke *et al.*, 2016; Seo *et al.*, 2017;
394 Ngugi and Stingl, 2018).
395
396 Regardless of variations in season, estuary type (North Bay is river-dominated versus South Bay,
397 which is more of a marine lagoon), or taxonomic group (e.g. *Proteobacteria*, *Actinobaceria,*
398 SAR11), a distinct brackish community emerges at the OTU level. Previous studies have posited
399 that distinct brackish microbial communities arise in systems where bacterial doubling rates are
400 faster than water residence times (Crump *et al.*, 2004; Herlemann *et al.*, 2011). Given the
401 variety of seasons and systems sampled, the findings of our study suggest that defined brackish
402 communities may also arise over shorter time scales and survive in waters with a variety of
403 water residence times. A recent, high-resolution daily time series found that coastal microbial
404 communities are constantly and quickly changing, with rapid transitions between distinct but
405 transient communities as coastal conditions change (Martin-Platero *et al.*, 2018). The
406 apparently robust and defined estuarine communities along the salinity gradient observed in
407 our dataset suggest that communities have adapted to a specific salinity regime and may be
408 capable of quickly transitioning with changing salinity gradient structures. Our study strongly
409 supports previous findings that distinct brackish bacterial communities exist and that closely
410 related organisms specialize/adapt to distinct salinity regimes (Herlemann *et al.*, 2011; Liu *et*
411 *al.*, 2015; Mehrshad *et al.*, 2016). Despite the unprecedented spatiotemporal sampling (and
412 sequencing) of SFB pelagic communities in this study, more fine-scale temporal sampling is

necessary to confirm how rapidly communities shift with changing salinity gradient structure and to tease apart if communities are ephemeral (quickly turning over) or if residence times are generally long enough to allow for distinct estuarine communities to develop regularly in SFB.

EXPERIMENTAL PROCEDURES

Sampling and DNA extraction. Bacterioplankton and archaeoplankton biomass was collected for DNA extraction approximately monthly between April 2012 and March 2014 during USGS Water quality monitoring cruises (https://sfbay.wr.usgs.gov/access/wqdata/index.html) in the channel of the San Francisco Bay estuary. Microbial cells were collected from bottom waters (1m above estuary floor) by pressure-filtering 150-1000mL of water from CTD casts through a 10-µm pore size polycarbonate Isopore membrane filter (47-mm diameter; EMD Millipore, Darmstadt, Germany) in line with a 0.22 µm polyethersulfone Supor-200 membrane filter (47-mm diameter; Pall, Port Washington, NY), followed by flash freezing on liquid nitrogen prior to storage at -80°C. Only 0.22 µm filters were frozen at -80°C and saved for extraction. DNA was extracted with the FastDNA SPIN Kit for Soil (MP Biomedicals, Santa Ana, CA), following the manufacturer's instructions, with the following modifications: bead tubes were homogenized for 40 seconds at speed 6.0 in a FastPrep bead beater, and final DNA was eluted into 75 µL 55°C sterile DNase-free water. DNA was quantified using the Qubit dsDNA Broad Range assay (Life Technologies, Grand Island, NY). DNA was stored at -80°C.

Environmental Data. Corresponding water quality data from sampling cruises was downloaded from the USGS San Francisco Bay Water Quality and California Day Flow websites, available at

434 the following links: (https://sfbay.wr.usgs.gov/access/wqdata/query/index.html and
435 http://www.water.ca.gov/dayflow/). Additional ammonium, nitrate, and nitrite measurements
436 were made using filtered (0.2 µm pore size) water that was frozen on dry ice prior to storage at
437 -20°C. Ammonium was measured using the salicylate-hypochlorite method (Bower and Holm-
438 Hansen, 1980). Nitrate and nitrite were measured using a SmartChem200 Discrete Analyzer
439 (Unity Scientific, Brookfield, CT) following standard procedures. Nutrients were measured
440 within one week of sample collection.
441
442 **Sequencing**. Through a DOE Joint Genome Institute (JGI) Community Science Program (CSP)
443 project, we have assembled 348 16S rRNA Illumina amplicon libraries from bottom water
444 samples (collected 1m above the estuary floor) on 20 approximately monthly cruises at 12
445 USGS monitoring stations spanning a 150 km transect (Fig. 1). In total, 174 samples were
446 sequenced with both new 16S V4 primers (Apprill *et al.*, 2015; Walters *et al.*, 2016) (515F-Y
447 GTGYCAGCMGCCGCGGTAA and 806RB GGACTACNVGGGTWTCTAAT) and 16S V4-V5 primers
448 (Parada *et al.*, 2016) (515F-Y and 926R CCGYCAATTYMTTTRAGTTT) and were included in the
449 following analyses. Samples were pooled and sequenced on an Illumina MiSeq. Sequences are
450 available on NCBI SRA under the BioProject PRJNA577706.
451
452 **Data Processing.** Raw reads were processed by JGI using the iTagger v2.2 method
453 (https://bitbucket.org/berkeleylab/jgi_itagger), which uses Usearch (Edgar, 2010), MAFFT
454 (Katoh *et al.*, 2002) and QIIME (Caporaso *et al.*, 2010). Reads were clustered at decreasing
455 levels of identity until the 97% cutoff to create OTUs. Low abundance sequences were not used

456 to cluster and were later mapped back to cluster centroids. Cluster centroid sequences were
457 evaluated with the reference database SILVA 128.
458
459 In general, amplicon library processing followed established protocols for filtering low
460 abundance reads, transforming read counts, and normalizing library sizes (McMurdie and
461 Holmes, 2014; Callahan *et al.*, 2016). To prevent high-variance-low-abundance OTUs from
462 strongly influencing downstream analyses, OTUs with less than 16 reads occurring in less than 3
463 samples were removed from libraries. Libraries were normalized in two ways depending on the
464 analysis, either through transforming counts to relative abundances or using the DESeq2
465 method, which uses a variance stabilizing transformation to adjust counts based on variation in
466 library size, and transformed using a geometric mean to account for large variation in OTU
467 counts (McMurdie and Holmes, 2014). Similar results were yielded with rarefied data (data not
468 shown). All analyses were conducted with R using primarily *phyloseq* (McMurdie and Holmes,
469 2013, 2014; Callahan *et al.*, 2016) and *vegan* (Oksanen *et al.*, 2018). Richness was calculated for
470 unfiltered amplicon libraries and libraries with OTUs filtered at a cutoff of greater than 15 reads
471 in greater than 2 samples, yielding similar results [data not shown]. Beta diversity metrics using
472 Bray-Curtis dissimilarity were calculated for VST or relative abundance transformed libraries.
473
474 Environmental data was centered and scaled prior to correlation testing (*scale*, *cor.test*, and
475 *ggpairs* functions). The natural log was used to transform variables where values ranged several
476 orders of magnitude (e.g. suspended particulate matter, chlorophyll). Samples were assigned
477 into salinity zones defined as fresh, oligohaline, mesohaline, polyhaline, and euhaline (Venice

478 system, (Battaglia, 1959)). The wet season was defined as December through May and the dry
479 season as June through November.
480
481 **Community Diversity Analysis.** Alpha and beta diversity measures were performed using
482 *phyloseq* and *vegan*. Heatmaps were made using Bray-Curtis dissimilarity and the *pheatmaps*
483 function. Friedman-Rafsky tests were used to test for graph-based sample segregation between
484 samples factored by salinity regime (fresh, oligohaline, mesohaline, polyhaline, or euhaline) and
485 based on Jaccard distance and Bray-Curtis dissimilarity between samples. Pure edges were
486 defined for samples within the same level (fresh, oligohaline, mesohaline, etc.). Edges were
487 defined using skeleton graphs including a minimum spanning tree (MST), distance threshold
488 (max jaccard distance = 0.4), and k-nearest neighbors (k=1.) Graphs were made using *igraph*,
489 *ggnetwork* and *phyloseqGraph Test* libraries. Differential abundance was analyzed through
490 DESeq2 using VST libraries. Principal coordinates analyses (PCoAs) use Bray-Curtis dissimilarity
491 and the V4 dataset unless otherwise noted. The *clusGap* function was used to calculate the gap
492 statistic for "goodness of clusters". Analysis of variance of ordinations was calculated using the
493 *adonis* function. Procrustes tests were used to compare ordinations quantitatively using the
494 *protest* function [*vegan*], which rotates and stretches ordinations until the distance between
495 corresponding points is minimized. M^2 represents one minus the squared correlation
496 coefficient (R) between the coordinates of corresponding points between the two ordinations
497 being tested. Differential abundance was analyzed through DESeq2 using VST libraries.
498 Nestedness versus turnover components of beta diversity analyses were calculated using the
499 *betapart* function and Bray-Curtis dissimilarity.

Nestedness of samples was calculated using the NODF statistic (Nestedness metric based on Overlap and Decreasing Fill), which describes combined column and row nestedness based on decreasing fill and paired overlap of presence data in a matrix (Almeida-Neto *et al.*, 2008). To calculate NODF, count tables were converted to a presence absence matrix and ordered by decreasing row sums, then decreasing column sums (decreasing prevalence and decreasing richness, respectively). The *oecosimu* function [*vegan*] was used to calculate the NODF statistic, which approximates the average percent of taxa from less diverse samples that occur in more diverse samples. The null model used was the "c0" model, which holds constant the column sums (sample richness) but allows row sums to vary (phyla prevalence) from the original data. Significance testing was based on default for *oecosimu* package and set to test if data values were greater than the null model. Entropy was calculated using the *diversity* function [*vegan*] and defined as the Shannon index of specific taxa (instead of by sample). Entropy, nestedness, and ordinations analyses were conducted using the full dataset and also using a random subsampling of samples evenly distributed across the five salinity zones (fresh, oligohaline, mesohaline, polyhaline, and euhaline), yielding similar results.

Acknowledgements

Thank you to Jim Cloern and the Water Quality of San Francisco Bay monitoring group (including but not limited to Jessica Dyke, Amy Kleckner, and Jan Thompson) at USGS and the R/V *Polaris* crew for facilitating our participation in numerous cruises. This work was funded by NSF CAREER grant OCE-0847266 from the Biological Oceanography program (to CAF), the

Stanford McGee research grant (JD), and NSF GRFP and Amherst College Fellowships (to ANR). The work conducted by the U.S. Department of Energy Joint Genome Institute, a DOE Office of Science User Facility, is supported by the Office of Science of the U.S. Department of Energy under Contract No. DE-AC02-05CH11231. Sequencing thanks to JGI CSP project 503022 to CAF. Special thanks to Tijana Glavino del Rio at JGI.

Conflict of Interest

The authors declare no conflict of interest.

References

Aguirre, M., Abad, D., Albaina, A., Cralle, L., Goñi-Urriza, M.S., Estonba, A., and Zarraonaindia, I. (2017) Unraveling the environmental and anthropogenic drivers of bacterial community changes in the Estuary of Bilbao and its tributaries. *PLOS ONE* **12**: e0178755.

Ahlgren, N.A., Chen, Y., Needham, D.M., Parada, A.E., Sachdeva, R., Trinh, V., et al. (2017) Genome and epigenome of a novel marine Thaumarchaeota strain suggest viral infection, phosphorothioation DNA modification and multiple restriction systems. *Environ Microbiol* **19**: 2434–2452.

Almeida-Neto, M., Guimarães, P., Guimarães, P.R., Loyola, R.D., and Ulrich, W. (2008) A consistent metric for nestedness analysis in ecological systems: reconciling concept and measurement. *Oikos* **117**: 1227–1239.

Alonso, C., Warnecke, F., Amann, R., and Pernthaler, J. (2007) High local and global diversity of Flavobacteria in marine plankton. *Environ Microbiol* **9**: 1253–1266.

Apprill, A., McNally, S., Parsons, R., and Weber, L. (2015) Minor revision to V4 region SSU rRNA 806R gene primer greatly increases detection of SAR11 bacterioplankton. *Aquat Microb Ecol* **75**:.

Battaglia, B. (1959) Final resolution of the symposium on the classification of brackish waters. *Archo Oceanogr Limnol* **11(suppl)**: 243–8.

Beck, M.W., Jabusch, T.W., Trowbridge, P.R., and Senn, D.B. (2018) Four decades of water quality change in the upper San Francisco Estuary. *Estuar Coast Shelf Sci* **212**: 11–22.

Bennke, C.M., Krüger, K., Kappelmann, L., Huang, S., Gobet, A., Schüler, M., et al. (2016) Polysaccharide utilisation loci of Bacteroidetes from two contrasting open ocean sites in the North Atlantic. *Environ Microbiol* **18**: 4456–4470.

Blainey, P.C., Mosier, A.C., Potanina, A., Francis, C.A., and Quake, S.R. (2011) Genome of a Low-Salinity Ammonia-Oxidizing Archaeon Determined by Single-Cell and Metagenomic Analysis. *PLOS ONE* **6**: e16626.

Bouvier, T.C. and Giorgio, P.A. del (2002) Compositional changes in free-living bacterial communities along a salinity gradient in two temperate estuaries. *Limnol Oceanogr* **47**: 453–470.

Callahan, B.J., Sankaran, K., Fukuyama, J.A., McMurdie, P.J., and Holmes, S.P. (2016) Bioconductor workflow for microbiome data analysis: from raw reads to community analyses. *F1000Research* **5**: 1492.

Campbell, B.J. and Kirchman, D.L. (2013) Bacterial diversity, community structure and potential growth rates along an estuarine salinity gradient. *ISME J* **7**: 210–220.

Caporaso, J.G., Kuczynski, J., Stombaugh, J., Bittinger, K., Bushman, F.D., Costello, E.K., et al. (2010) QIIME allows analysis of high-throughput community sequencing data. *Nat Methods* **7**: 335–336.

Cloern, J.E. (2001) Our evolving conceptual model of the coastal eutrophication problem. *Mar Ecol Prog Ser* **210**: 223–253.

Cloern, J.E. (2019) Patterns, pace, and processes of water-quality variability in a long-studied estuary. *Limnol Oceanogr* **64**: S192–S208.

Cloern, J.E. (1996) Phytoplankton bloom dynamics in coastal ecosystems: A review with some general lessons from sustained investigation of San Francisco Bay, California. *Rev Geophys* **34**: 127–168.

Cloern, J.E. (1987) Turbidity as a control on phytoplankton biomass and productivity in estuaries. *Cont Shelf Res* **7**: 1367–1381.

Cloern, J.E. and Dufford, R. (2005) Phytoplankton community ecology: principles applied in San Francisco Bay. *Mar Ecol Prog Ser* **285**: 11–28.

Cloern, J.E. and Jassby, A.D. (2012) Drivers of change in estuarine-coastal ecosystems: Discoveries from four decades of study in San Francisco Bay. *Rev Geophys* **50**: RG4001.

Cloern, J.E. and Jassby, A.D. (2010) Patterns and Scales of Phytoplankton Variability in Estuarine–Coastal Ecosystems. *Estuaries Coasts* **33**: 230–241.

Cloern, J.E., Jassby, A.D., Schraga, T.S., Nejad, E., and Martin, C. (2017) Ecosystem variability along the estuarine salinity gradient: Examples from long-term study of San Francisco Bay. *Limnol Oceanogr* **62**: S272–S291.

Crump, B.C., Armbrust, E.V., and Baross, J.A. (1999) Phylogenetic Analysis of Particle-Attached and Free-Living Bacterial Communities in the Columbia River, Its Estuary, and the Adjacent Coastal Ocean. *Appl Environ Microbiol* **65**: 3192–3204.

Crump, B.C., Hopkinson, C.S., Sogin, M.L., and Hobbie, J.E. (2004) Microbial Biogeography along an Estuarine Salinity Gradient: Combined Influences of Bacterial Growth and Residence Time. *Appl Environ Microbiol* **70**: 1494–1505.

Damashek, J., Casciotti, K.L., and Francis, C.A. (2016) Variable Nitrification Rates Across Environmental Gradients in Turbid, Nutrient-Rich Estuary Waters of San Francisco Bay. *Estuaries Coasts* **39**: 1050–1071.

Doherty, M., Yager, P.L., Moran, M.A., Coles, V.J., Fortunato, C.S., Krusche, A.V., et al. (2017) Bacterial Biogeography across the Amazon River-Ocean Continuum. *Front Microbiol* **8**:.

Edgar, R.C. (2010) Search and clustering orders of magnitude faster than BLAST. *Bioinformatics* **26**: 2460–2461.

Fortunato, C.S. and Crump, B.C. (2011) Bacterioplankton Community Variation Across River to Ocean Environmental Gradients. *Microb Ecol* **62**: 374–382.

Fortunato, C.S., Eiler, A., Herfort, L., Needoba, J.A., Peterson, T.D., and Crump, B.C. (2013) Determining indicator taxa across spatial and seasonal gradients in the Columbia River coastal margin. *ISME J* **7**: 1899–1911.

Fortunato, C.S., Herfort, L., Zuber, P., Baptista, A.M., and Crump, B.C. (2012) Spatial variability overwhelms seasonal patterns in bacterioplankton communities across a river to ocean gradient. *ISME J* **6**: 554–563.

Ghai, R., Mizuno, C.M., Picazo, A., Camacho, A., and Rodriguez-Valera, F. (2014) Key roles for freshwater Actinobacteria revealed by deep metagenomic sequencing. *Mol Ecol* **23**: 6073–6090.

Ghai, R., Mizuno, C.M., Picazo, A., Camacho, A., and Rodriguez-Valera, F. (2013) Metagenomics uncovers a new group of low GC and ultra-small marine Actinobacteria. *Sci Rep* **3**: srep02471.

Glöckner, F.O., Zaichikov, E., Belkova, N., Denissova, L., Pernthaler, J., Pernthaler, A., and Amann, R. (2000) Comparative 16S rRNA Analysis of Lake Bacterioplankton Reveals Globally Distributed Phylogenetic Clusters Including an Abundant Group of Actinobacteria. *Appl Env Microbiol* **66**: 5053–5065.

Gómez-Pereira, P.R., Fuchs, B.M., Alonso, C., Oliver, M.J., van Beusekom, J.E.E., and Amann, R. (2010) Distinct flavobacterial communities in contrasting water masses of the North Atlantic Ocean. *ISME J* **4**: 472–487.

Happel, E., Bartl, I., Voss, M., and Riemann, L. (2018) Extensive nitrification and active ammonia oxidizers in two contrasting coastal systems of the Baltic Sea. *Environ Microbiol* **20**: 2913–2926.

Henson, M.W., Lanclos, V.C., Faircloth, B.C., and Thrash, J.C. (2018) Cultivation and genomics of the first freshwater SAR11 (LD12) isolate. *ISME J* **12**: 1846–1860.

Herlemann, D.P., Labrenz, M., Jürgens, K., Bertilsson, S., Waniek, J.J., and Andersson, A.F. (2011) Transitions in bacterial communities along the 2000 km salinity gradient of the Baltic Sea. *ISME J* **5**: 1571–1579.

Herlemann, D.P.R., Woelk, J., Labrenz, M., and Jürgens, K. (2014) Diversity and abundance of “Pelagibacterales” (SAR11) in the Baltic Sea salinity gradient. *Syst Appl Microbiol* **37**: 601–604.

Hewson, I. and Fuhrman, J.A. (2004) Richness and Diversity of Bacterioplankton Species along an Estuarine Gradient in Moreton Bay, Australia. *Appl Env Microbiol* **70**: 3425–3433.

Hollibaugh, J., Gifford, S., Moran, M.A., Ross, M., Sharma, S., and Tolar, B. (2014) Seasonal variation in the metratranscriptomes of a Thaumarchaeota population from SE USA coastal waters. *ISME J* **8**: 685–698.

Hollibaugh, J.T. and Wong, P.S. (1999) Microbial processes in the San Francisco Bay estuarine turbidity maximum. *Estuaries* **22**: 848–862.

Hollibaugh, J.T., Wong, P.S., and Murrell, M.C. (2000) Similarity of particle-associated and free-living bacterial communities in northern San Francisco Bay, California. *Aquat Microb Ecol* **21**: 103–114.

Holmfeldt, K., Dziallas, C., Titelman, J., Pohlmann, K., Grossart, H.-P., and Riemann, L. (2009) Diversity and abundance of freshwater Actinobacteria along environmental gradients in the brackish northern Baltic Sea. *Environ Microbiol* **11**: 2042–2054.

Hu, A., Yang, Z., Yu, C.-P., and Jiao, N. (2013) Dynamics of Autotrophic Marine Planktonic Thaumarchaeota in the East China Sea. *PLoS ONE* **8**:.

Kan, J., Evans, S.E., Chen, F., and Suzuki, M.T. (2008) Novel estuarine bacterioplankton in rRNA operon libraries from the Chesapeake Bay. *Aquat Microb Ecol* **51**: 55–66.

Katoh, K., Misawa, K., Kuma, K., and Miyata, T. (2002) MAFFT: a novel method for rapid multiple sequence alignment based on fast Fourier transform. *Nucleic Acids Res* **30**: 3059–3066.

Kim, J.-G., Gwak, J.-H., Jung, M.-Y., An, S.-U., Hyun, J.-H., Kang, S., and Rhee, S.-K. (2019) Distinct temporal dynamics of planktonic archaeal and bacterial assemblages in the bays of the Yellow Sea. *PLOS ONE* **14**: e0221408.

Kimmerer, W. (2004) Open Water Processes of the San Francisco Estuary: From Physical Forcing to Biological Responses. *San Franc Estuary Watershed Sci* **2**:.

Kirchman, D.L., Dittel, A.I., Malmstrom, R.R., and Cottrell, M.T. (2005) Biogeography of major bacterial groups in the Delaware Estuary. *Limnol Oceanogr* **50**: 1697–1706.

Ladau, J. and Eloe-Fadrosh, E.A. (2019) Spatial, Temporal, and Phylogenetic Scales of Microbial Ecology. *Trends Microbiol* **0**:

Li, J., Jiang, X., Jing, Z., Li, G., Chen, Z., Zhou, L., et al. (2017) Spatial and seasonal distributions of bacterioplankton in the Pearl River Estuary: The combined effects of riverine inputs, temperature, and phytoplankton. *Mar Pollut Bull* **125**: 199–207.

Liu, J., Fu, B., Yang, H., Zhao, M., He, B., and Zhang, X.-H. (2015) Phylogenetic shifts of bacterioplankton community composition along the Pearl Estuary: the potential impact of hypoxia and nutrients. *Front Microbiol* **6**:.

Liu, J., Yu, S., Zhao, M., He, B., and Zhang, X.-H. (2014) Shifts in archaeaplankton community structure along ecological gradients of Pearl Estuary. *FEMS Microbiol Ecol* **90**: 424–435.

Lozupone, C.A. and Knight, R. (2007) Global patterns in bacterial diversity. *Proc Natl Acad Sci* **104**: 11436–11440.

Lucas, L.V., Cloern, J.E., Koseff, J.R., Monismith, S.G., and Thompson, J.K. (1998) Does the Sverdrup critical depth model explain bloom dynamics in estuaries? *J Mar Res* **56**: 375–415.

Lucas, L.V., Koseff, J.R., Monismith, S.G., and Thompson, J.K. (2009) Shallow water processes govern system-wide phytoplankton bloom dynamics: A modeling study. *J Mar Syst* **75**: 70–86.

Martin-Platero, A.M., Cleary, B., Kauffman, K., Preheim, S.P., McGillicuddy, D.J., Alm, E.J., and Polz, M.F. (2018) High resolution time series reveals cohesive but short-lived communities in coastal plankton. *Nat Commun* **9**: 266.

Mason, O.U., Canter, E.J., Gillies, L.E., Paisie, T.K., and Roberts, B.J. (2016) Mississippi River Plume Enriches Microbial Diversity in the Northern Gulf of Mexico. *Front Microbiol* **7**:.

McMurdie, P.J. and Holmes, S. (2013) phyloseq: An R Package for Reproducible Interactive Analysis and Graphics of Microbiome Census Data. *PLOS ONE* **8**: e61217.

McMurdie, P.J. and Holmes, S. (2014) Waste Not, Want Not: Why Rarefying Microbiome Data Is Inadmissible. *PLOS Comput Biol* **10**: e1003531.

Mehrshad, M., Amoozegar, M.A., Ghai, R., Fazeli, S.A.S., and Rodriguez-Valera, F. (2016) Genome Reconstruction from Metagenomic Data Sets Reveals Novel Microbes in the Brackish Waters of the Caspian Sea. *Appl Environ Microbiol* **82**: 1599–1612.

Mizuno, C.M., Rodriguez-Valera, F., and Ghai, R. (2015) Genomes of Planktonic Acidimicrobiales: Widening Horizons for Marine Actinobacteria by Metagenomics. *mBio* **6**: e02083-14.

Mosier, A.C., Lund, M.B., and Francis, C.A. (2012) Ecophysiology of an ammonia-oxidizing archaeon adapted to low-salinity habitats. *Microb Ecol* **64**: 955–963.

Murray, A.E., Hollibaugh, J.T., and Orrego, C. (1996) Phylogenetic compositions of bacterioplankton from two California estuaries compared by denaturing gradient gel electrophoresis of 16S rDNA fragments. *Appl Environ Microbiol* **62**: 2676–2680.

Murrell, M.C., Hollibaugh, J.T., Silver, M.W., and Wong, P.S. (1999) Bacterioplankton dynamics in northern San Francisco Bay: Role of particle association and seasonal freshwater flow. *Limnol Oceanogr* **44**: 295–308.

Ngugi, D.K. and Stingl, U. (2018) High-Quality Draft Single-Cell Genome Sequence of the NS5 Marine Group from the Coastal Red Sea. *Genome Announc* **6**: e00565-18.

Nichols, F.H., Cloern, J.E., Luoma, S.N., and Peterson, D.H. (1986) The Modification of an Estuary. *Science* **231**: 567–573.

Oksanen, J., Blanchet, F.G., Friendly, M., Kindt, R., Legendre, P., McGlinn, D., et al. (2018) vegan: Community Ecology Package.

Parada, A.E., Needham, D.M., and Fuhrman, J.A. (2016) Every base matters: assessing small subunit rRNA primers for marine microbiomes with mock communities, time series and global field samples. *Environ Microbiol* **18**: 1403–1414.

Pitcher, A., Wuchter, C., Siedenberg, K., Schouten, S., and Sinninghe Damsté, J.S. (2011) Crenarchaeol tracks winter blooms of ammonia-oxidizing Thaumarchaeota in the coastal North Sea. *Limnol Oceanogr* **56**: 2308–2318.

Raimonet, M. and Cloern, J.E. (2017) Estuary–ocean connectivity: fast physics, slow biology. *Glob Change Biol* **23**: 2345–2357.

Santoro, A.E., Dupont, C.L., Richter, R.A., Craig, M.T., Carini, P., McIlvin, M.R., et al. (2015) Genomic and proteomic characterization of “Candidatus Nitrosopelagicus brevis”: An ammonia-oxidizing archaeon from the open ocean. *Proc Natl Acad Sci* **112**: 1173–1178.

Satinsky, B.M., Crump, B.C., Smith, C.B., Sharma, S., Zielinski, B.L., Doherty, M., et al. (2014) Microspatial gene expression patterns in the Amazon River Plume. *Proc Natl Acad Sci* **111**: 11085–11090.

Schaefer, S.C. and Hollibaugh, J.T. (2017) Temperature Decouples Ammonium and Nitrite Oxidation in Coastal Waters. *Environ Sci Technol*.

Schraga, T.S. and Cloern, J.E. (2017) Water quality measurements in San Francisco Bay by the U.S. Geological Survey, 1969–2015. *Sci Data* **4**: 170098.

Seo, J.-H., Kang, I., Yang, S.-J., and Cho, J.-C. (2017) Characterization of spatial distribution of the bacterial community in the South Sea of Korea. *PLoS ONE* **12**:.

Smith, M.W., Herfort, L., Fortunato, C.S., Crump, B.C., and Simon, H.M. (2017) Microbial players and processes involved in phytoplankton bloom utilization in the water column of a fast-flowing, river-dominated estuary. *MicrobiologyOpen* **6**: e00467.

Stepanauskas, R., Moran, M.A., Bergamaschi, B.A., and Hollibaugh, J.T. (2003) Covariance of bacterioplankton composition and environmental variables in a temperate delta system. *Aquat Microb Ecol* **31**: 14.

Sutula, M., Kudela, R., Hagy, J.D., Harding, L.W., Senn, D., Cloern, J.E., et al. (2017) Novel analyses of long-term data provide a scientific basis for chlorophyll-a thresholds in San Francisco Bay. *Estuar Coast Shelf Sci* **197**: 107–118.

Thompson, L.R., Sanders, J.G., McDonald, D., Amir, A., Ladau, J., Locey, K.J., et al. (2017) A communal catalogue reveals Earth's multiscale microbial diversity. *Nature* **551**: 457–463.

Vergin, K.L., Beszteri, B., Monier, A., Cameron Thrash, J., Temperton, B., Treusch, A.H., et al. (2013) High-resolution SAR11 ecotype dynamics at the Bermuda Atlantic Time-series Study site by phylogenetic placement of pyrosequences. *ISME J* **7**: 1322–1332.

Walters, R.A., Cheng, R.T., and Conomos, T.J. (1985) Time scales of circulation and mixing processes of San Francisco Bay waters. *Hydrobiologia* **129**: 24.

Walters, W., Hyde, E.R., Berg-Lyons, D., Ackermann, G., Humphrey, G., Parada, A., et al. (2016) Improved Bacterial 16S rRNA Gene (V4 and V4-5) and Fungal Internal Transcribed Spacer Marker Gene Primers for Microbial Community Surveys. *mSystems* **1**: e00009-15.

Wankel, S.D., Kendall, C., Francis, C.A., and Paytan, A. (2006) Nitrogen sources and cycling in the San Francisco Bay Estuary: A nitrate dual isotopic composition approach. *Limnol Oceanogr* **51**: 1654–1664.

Williams, T.J., Wilkins, D., Long, E., Evans, F., DeMaere, M.Z., Raftery, M.J., and Cavicchioli, R. (2013) The role of planktonic Flavobacteria in processing algal organic matter in coastal East Antarctica revealed using metagenomics and metaproteomics. *Environ Microbiol* **15**: 1302–1317.

Wuchter, C., Abbas, B., Coolen, M.J.L., Herfort, L., van Bleijswijk, J., Timmers, P., et al. (2006) Archaeal nitrification in the ocean. *Proc Natl Acad Sci U S A* **103**: 12317–12322.

Yang, C., Li, Y., Zhou, B., Zhou, Y., Zheng, W., Tian, Y., et al. (2015) Illumina sequencing-based analysis of free-living bacterial community dynamics during an *Akashiwo sanguine* bloom in Xiamen sea, China. *Sci Rep* **5**: 8476.

Zhang, Y., Jiao, N.Z., 焦念志, Cottrell, M.T., and Kirchman, D.L. (2006) Contribution of major bacterial groups to bacterial biomass production along a salinity gradient in the South China Sea.

Zou, D., Li, Y., Kao, S.-J., Liu, H., and Li, M. (2019) Genomic adaptation to eutrophication of ammonia-oxidizing archaea in the Pearl River estuary. *Environ Microbiol* **21**: 2320–2332.

Figures Captions

Fig. 1 Map of San Francisco Bay and USGS water quality stations sampled in this study (A) and tile plots of environmental variables, including salinity (B), temperature in °C (C), and suspended particulate matter (SPM) in mg/L (D). For (B-D) the x-axis corresponds to date of 20 approximately monthly cruises from April 2012 to March 2014 and y-axis to USGS station sampled going from Lower South Bay (36) to the Sacramento River (657).

Fig. 2 Beta diversity of the V4 dataset shown through PCoA plots based on Bray-Curtis dissimilarity for the V4 dataset. Whole bay ordinations include all 174 samples (A, B). North Bay ordinations only include samples from Stations 657 to 18 (C, D). And South Bay ordinations include samples from stations 24 through 36 (E, F). Point color is based on the environmental variable with the highest correlation (*r* value) with axis 1 (A, C, E) or axis 2 (B, D, F), respectively.

Fig. 3 Richness (# of OTUs) of microbial communities shown for all samples (A) with the x-axis corresponds to date of 20 approximately monthly cruises from April 2012 to March 2014 and the y-axis corresponding to station number going from Lower South Bay (36) to the Sacramento River (657). (B) shows the correlation of richness and SPM ($r^2 = 0.55$).

Fig. 4 Diversity metrics at different taxonomic levels. (A) The NODF statistic was used to measure nestedness of each sample and compared to a null model with constant column sums (sample richness) but changing rows (taxa prevalence). * indicate a value is greater than null NODF with a $p < 0.05$. (B) Entropy calculated as the Shannon index of taxa. Violin plots are scaled to have the same width and horizontal lines indicate the 50th quartile based on point distribution. (C) DESeq2 was used to calculate log2-fold change in taxa abundance across salinity zones. Only taxa with significant variation ($p < .001$) across salinity zones are included in plots.

Fig. 5 The % relative abundance of SAR11 families (A) and Cyanobacteria genera (B) at 6 stations representative for the five salinity zones and South Bay. High Thaumarchaeota abundance (C) corresponds with high nitrite concentrations in South Bay (D) ($r^2 = 0.79$). The y-axis shows the relative abundance of taxa in the whole community (A-C). The x-axis of each panel corresponds to date of 20 approximately monthly cruises from April 2012 to March 2014 and station is indicated at the top of the panel.

Figure 1

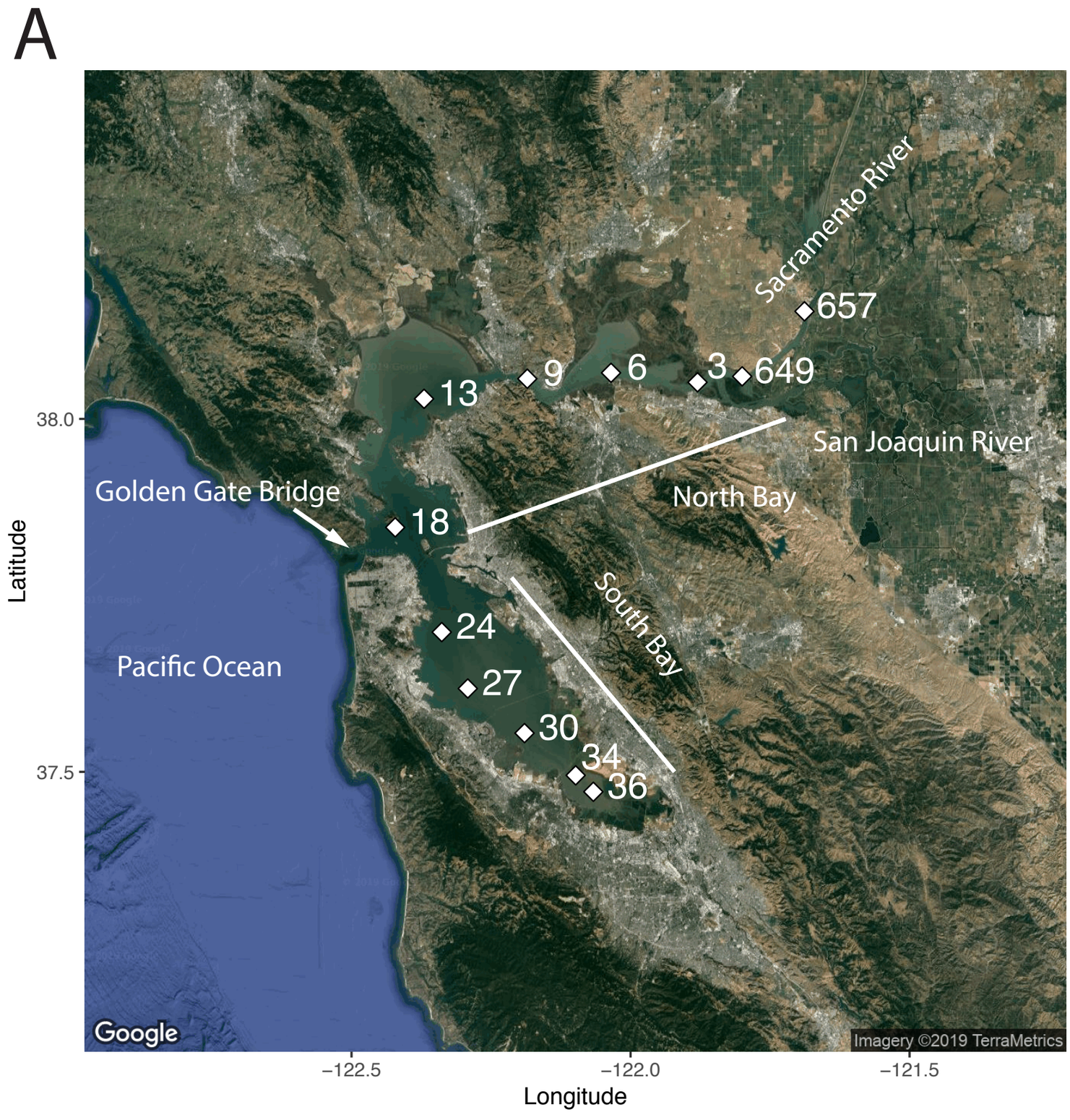
A
Sacramento River
657
649
3
6
9
13
18
24
27
30
34
36
San Joaquin River
North Bay
Golden Gate Bridge
South Bay
Pacific Ocean
Google
Imagery ©2019 TerraMetrics
38.0
37.5
Latitude
−122.5
−122.0
−121.5
Longitude

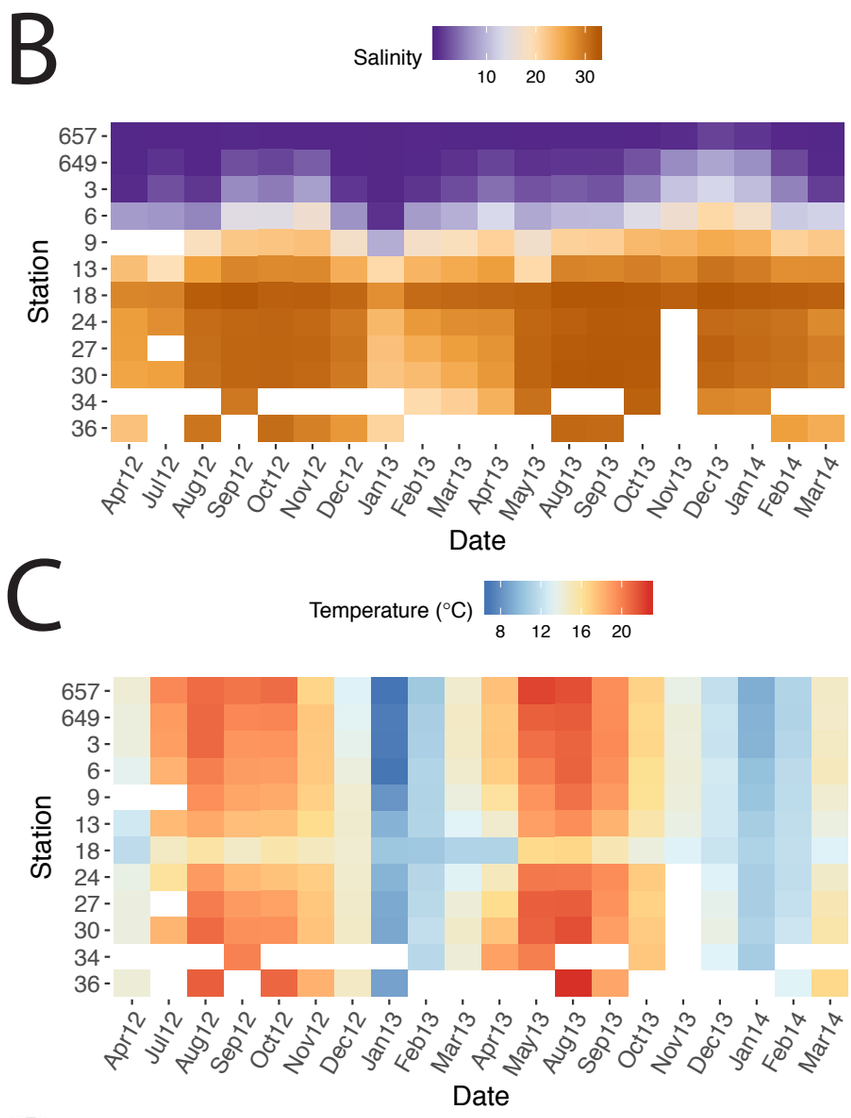
B
Salinity
10
20
30
Station
657
649
3
6
9
13
18
24
27
30
34
36
Apr12
Jul12
Aug12
Sep12
Oct12
Nov12
Dec12
Jan13
Feb13
Mar13
Apr13
May13
Aug13
Sep13
Oct13
Nov13
Dec13
Jan14
Feb14
Mar14
Date

C
Temperature (°C)
8
12
16
20
Station
657
649
3
6
9
13
18
24
27
30
34
36
Apr12
Jul12
Aug12
Sep12
Oct12
Nov12
Dec12
Jan13
Feb13
Mar13
Apr13
May13
Aug13
Sep13
Oct13
Nov13
Dec13
Jan14
Feb14
Mar14
Date

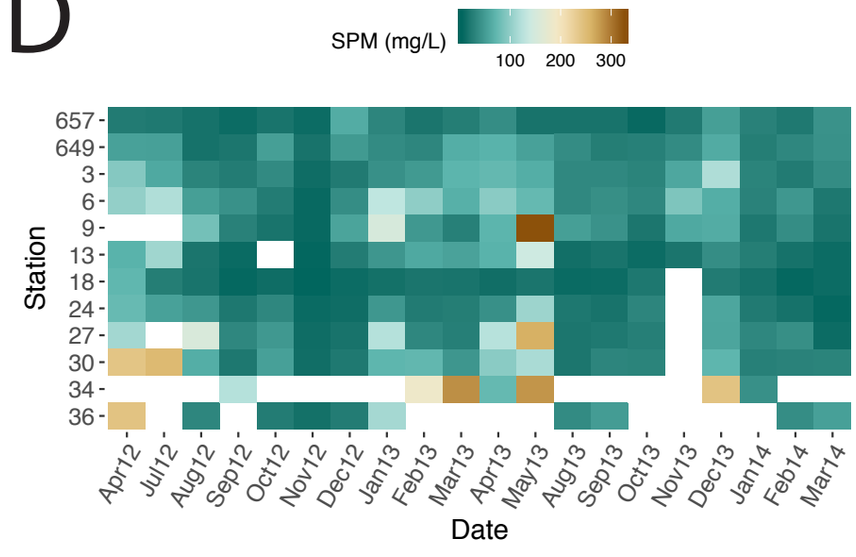
D
SPM (mg/L)
100
200
300
Station
657
649
3
6
9
13
18
24
27
30
34
36
Apr12
Jul12
Aug12
Sep12
Oct12
Nov12
Dec12
Jan13
Feb13
Mar13
Apr13
May13
Aug13
Sep13
Oct13
Nov13
Dec13
Jan14
Feb14
Mar14
Date

Figure 2

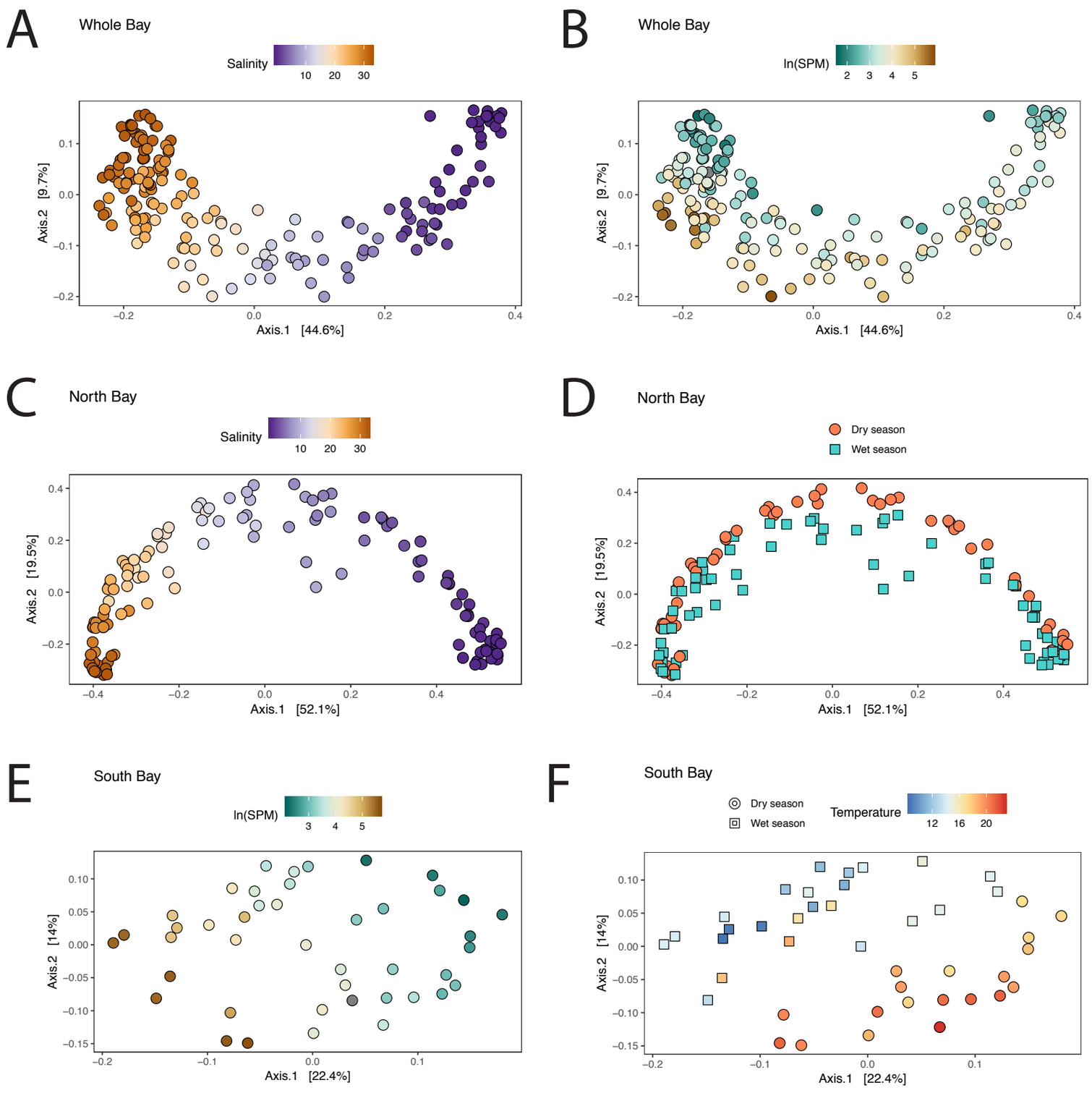
A
Whole Bay
Salinity
10 20 30
Axis.2 [9.7%]
Axis.1 [44.6%]
B
Whole Bay
ln(SPM)
2 3 4 5
Axis.2 [9.7%]
Axis.1 [44.6%]
C
North Bay
Salinity
10 20 30
Axis.2 [19.5%]
Axis.1 [52.1%]
D
North Bay
Dry season
Wet season
Axis.2 [19.5%]
Axis.1 [52.1%]
E
South Bay
ln(SPM)
3 4 5
Axis.2 [14%]
Axis.1 [22.4%]
F
South Bay
Dry season
Wet season
Temperature
12 16 20
Axis.2 [14%]
Axis.1 [22.4%]

Figure 3

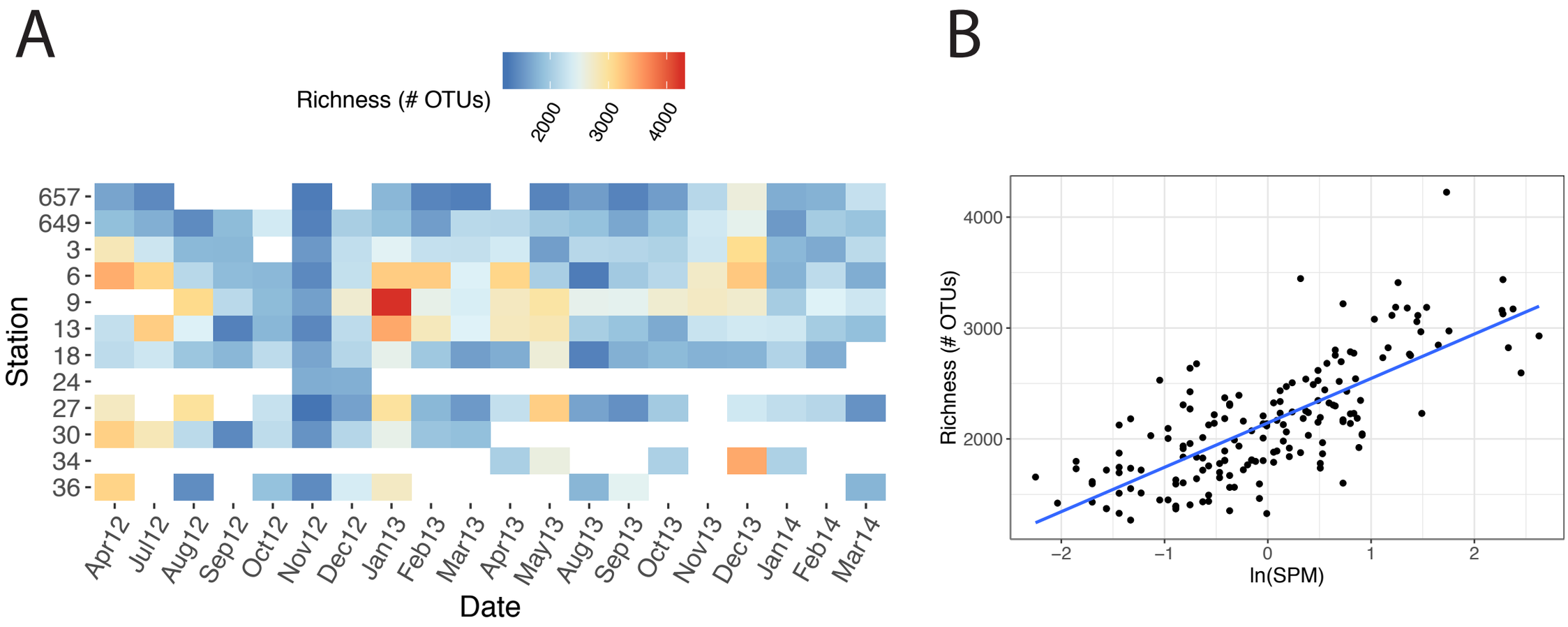
A
Richness (# OTUs)
2000
3000
4000
Station
657
649
3
6
9
13
18
24
27
30
34
36
Apr12
Jul12
Aug12
Sep12
Oct12
Nov12
Dec12
Jan13
Feb13
Mar13
Apr13
May13
Aug13
Sep13
Oct13
Nov13
Dec13
Jan14
Feb14
Mar14
Date
B
4000
3000
2000
Richness (# OTUs)
−2
−1
0
1
2
ln(SPM)

Figure 4

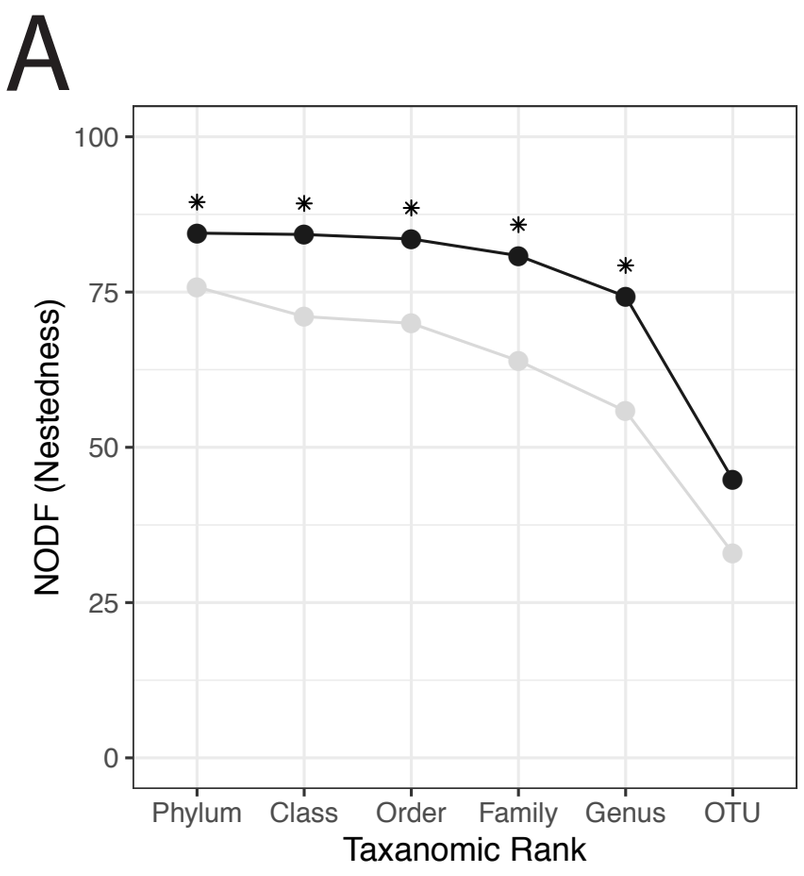
A
100
75
50
25
0
NODF (Nestedness)
Phylum
Class
Order
Family
Genus
OTU
Taxanomic Rank

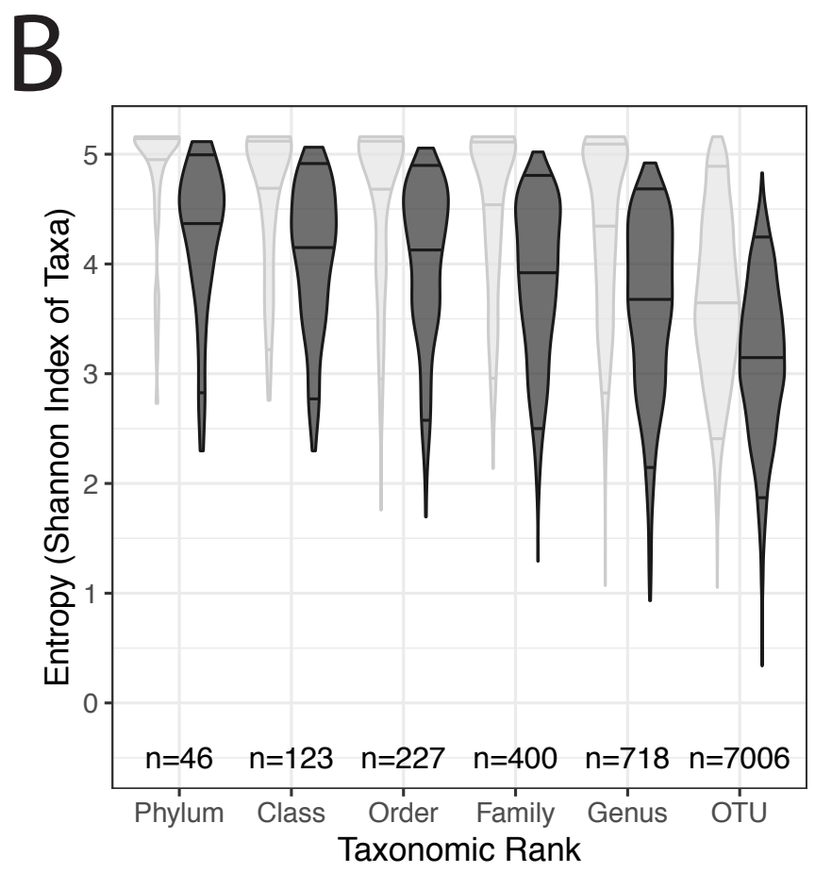
B
5
4
3
2
1
0
Entropy (Shannon Index of Taxa)
n=46
n=123
n=227
n=400
n=718
n=7006
Phylum
Class
Order
Family
Genus
OTU
Taxonomic Rank

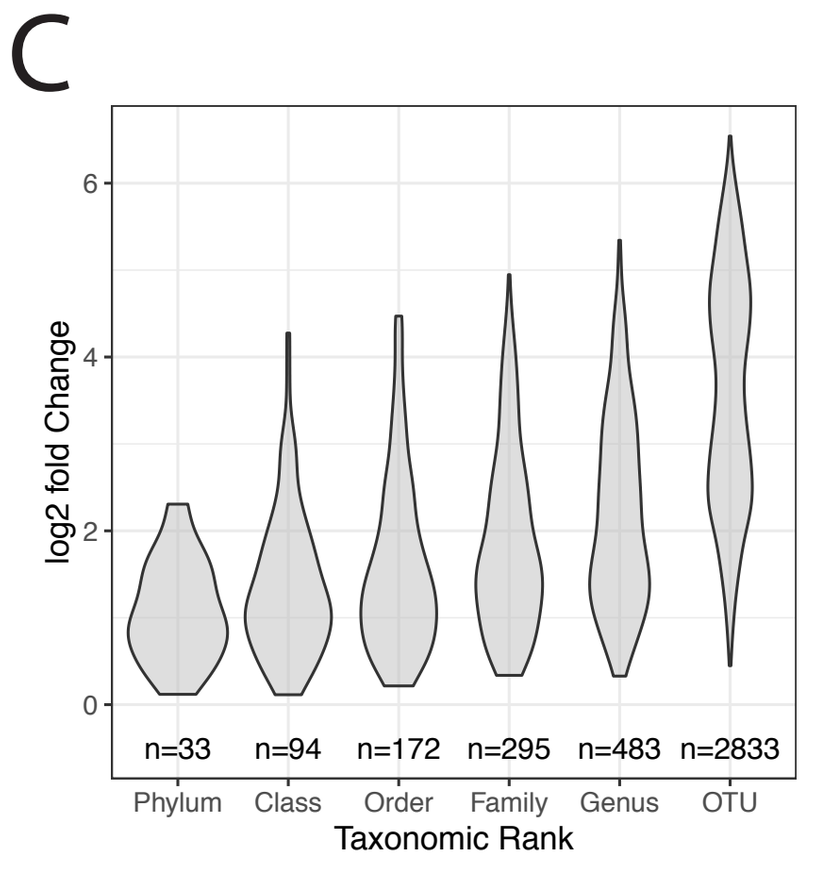
C
6
4
2
0
log2 fold Change
n=33
n=94
n=172
n=295
n=483
n=2833
Phylum
Class
Order
Family
Genus
OTU
Taxonomic Rank

Figure 5

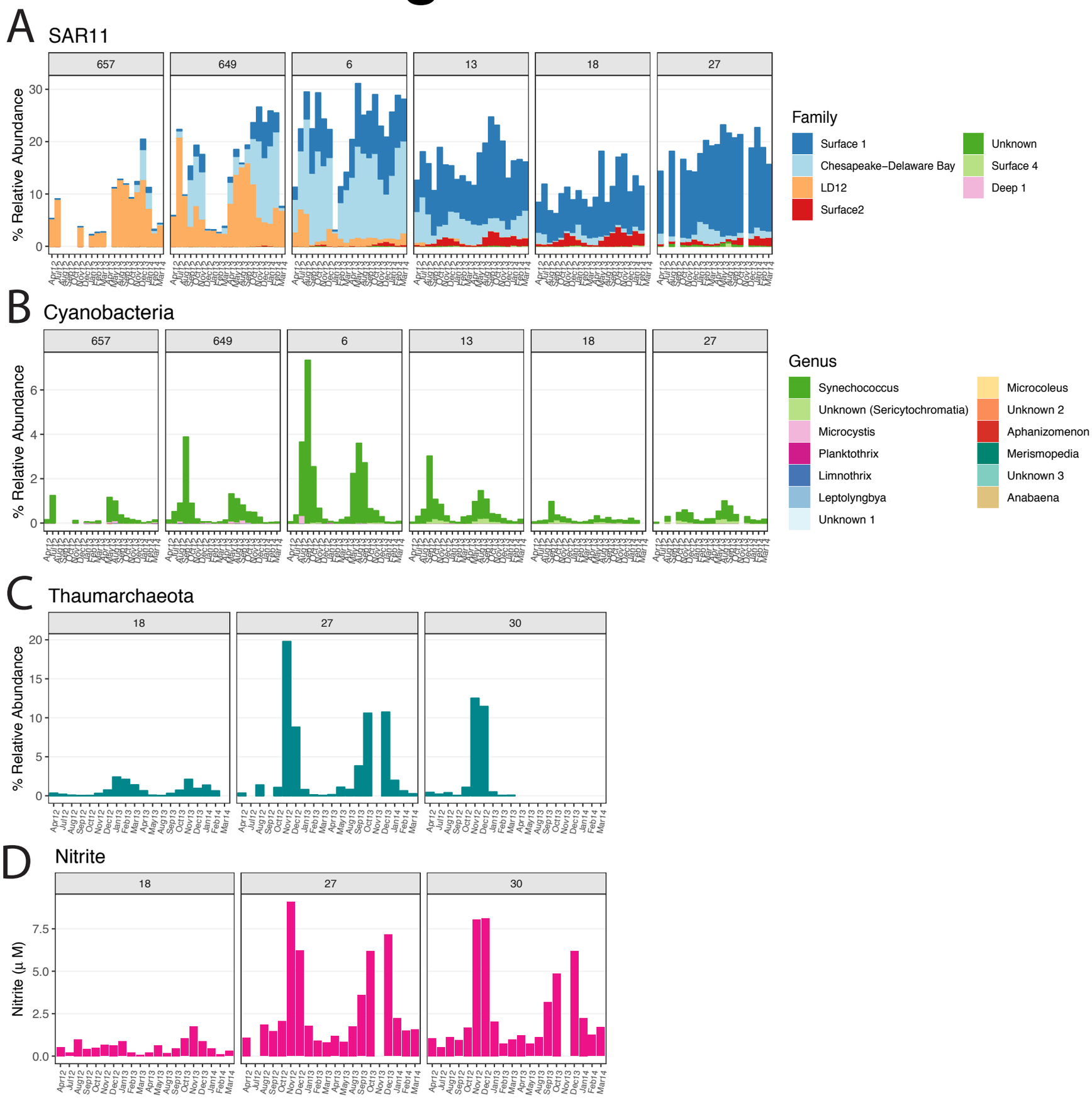
A
SAR11
657
649
6
13
18
27
% Relative Abundance
0
10
20
30
Family
Surface 1
Chesapeake−Delaware Bay
LD12
Surface2
Unknown
Surface 4
Deep 1
B
Cyanobacteria
% Relative Abundance
0
2
4
6
Genus
Synechococcus
Unknown (Sericytochromatia)
Microcystis
Planktothrix
Limnothrix
Leptolyngbya
Unknown 1
Microcoleus
Unknown 2
Aphanizomenon
Merismopedia
Unknown 3
Anabaena
C
Thaumarchaeota
18
27
30
% Relative Abundance
0
5
10
15
20
D
Nitrite
Nitrite (µ M)
0.0
2.5
5.0
7.5
Apr12
Jul12
Aug12
Sep12
Oct12
Nov12
Dec12
Jan13
Feb13
Mar13
Apr13
May13
Aug13
Sep13
Oct13
Nov13
Dec13
Jan14
Feb14
Mar14

Supplemental Information

Diversity metrics of pelagic archaeal and bacterial communities in San Francisco Bay depend on scale

Anna Rasmussen[1], Julian Damashek[1†], Emiley Eloe-Fadrosh[2], and Christopher A. Francis[1]*

[1]Department of Earth System Science, Stanford University, Stanford, CA 94305, USA

[2]Department of Energy Joint Genome Institute, Walnut Creek, California 94598, USA

*Correspondence: Christopher Francis, Department of Earth System Science, 473 Via Ortega, Y2E2 Bldg Rm 140, Stanford University, Stanford, CA 94305, USA. Email: caf@stanford.edu

Running Title: Pelagic bacteria and archaea of San Francisco Bay

List of Supporting Information

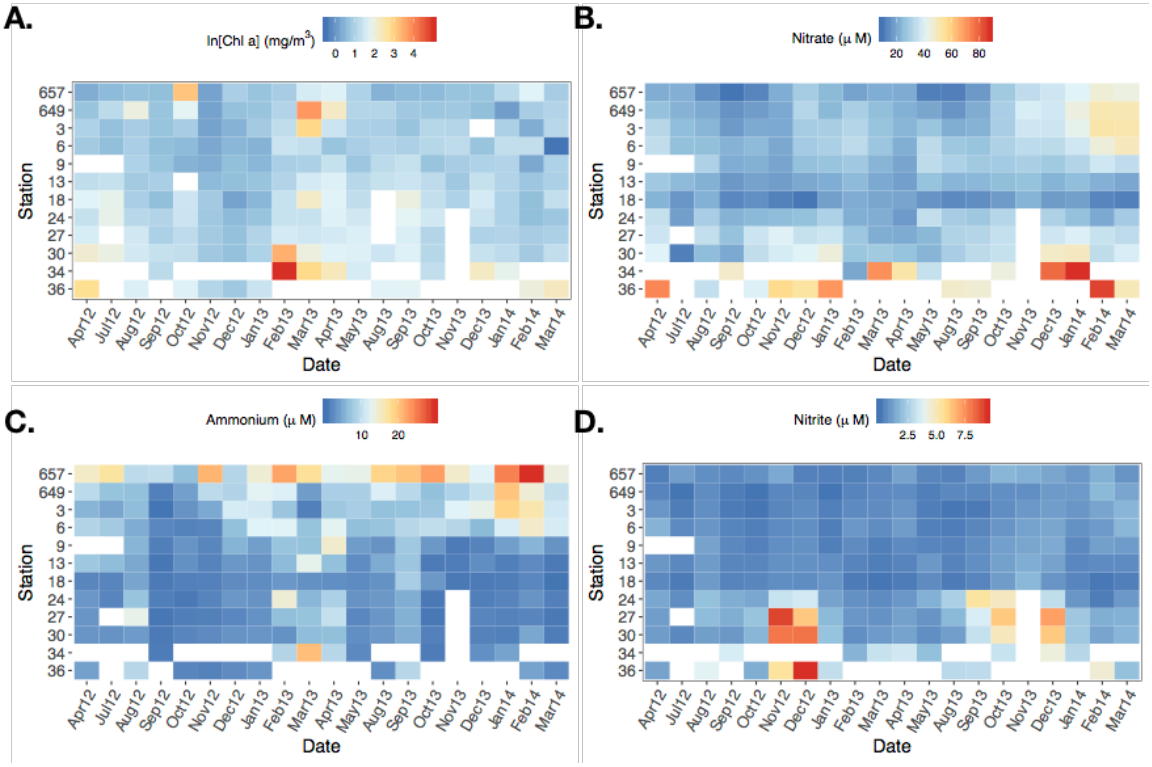

Fig. S1 Environmental data for the natural log of chlorophyll a (A), nitrate (B), ammonium (C), and nitrite (D). The x-axis corresponds to date of 20 approximately monthly cruises from April 2012 to March 2014 and the y-axis to USGS station sampled going from Lower South Bay (36) to the Sacramento River (657).

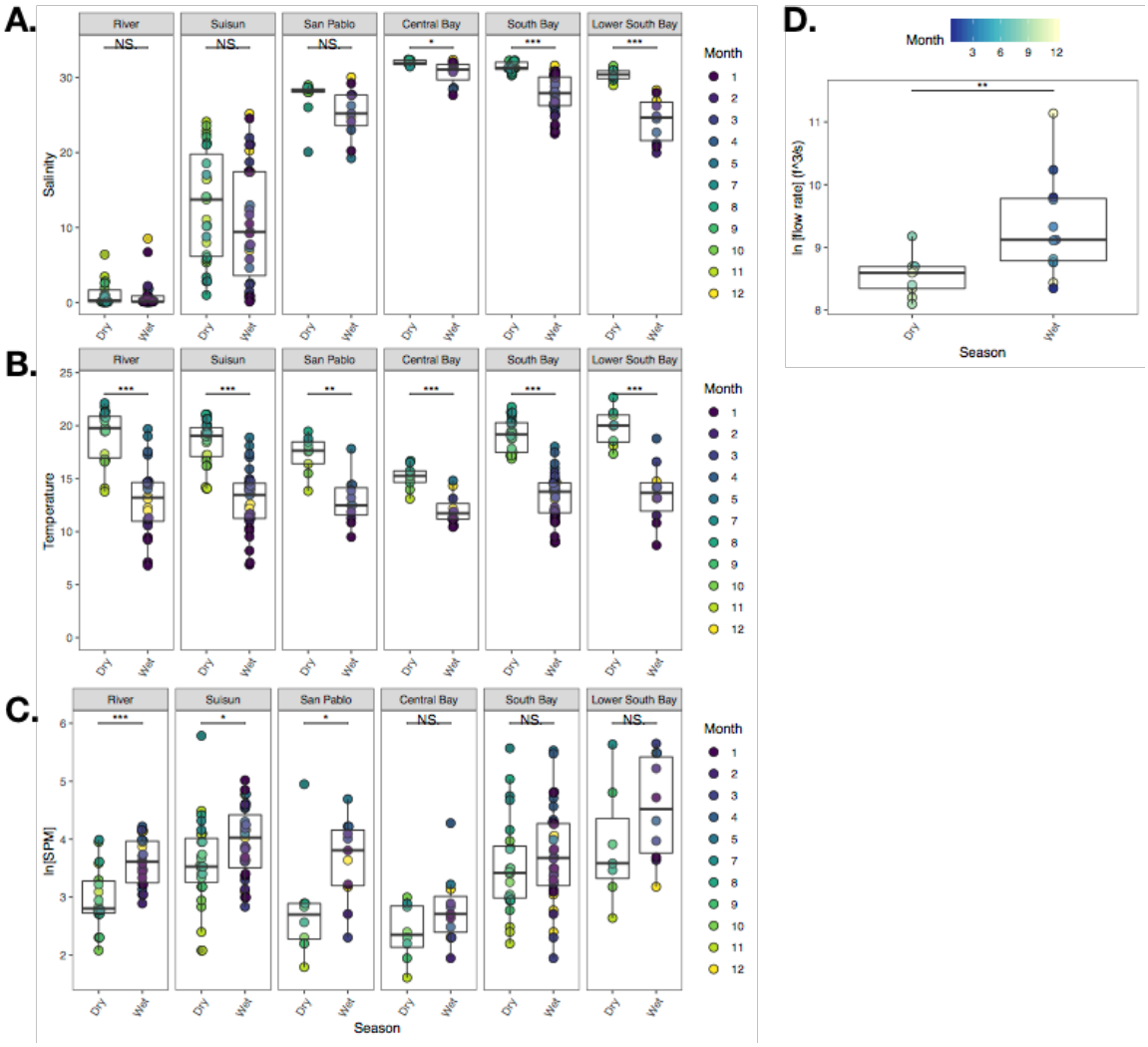

Fig. S2 Environmental variables shown in different regions of San Francisco Bay for wet and dry seasons. * indicate p-value < .05, ** p-value < .01, *** p-value <.001 and NS is not significant.

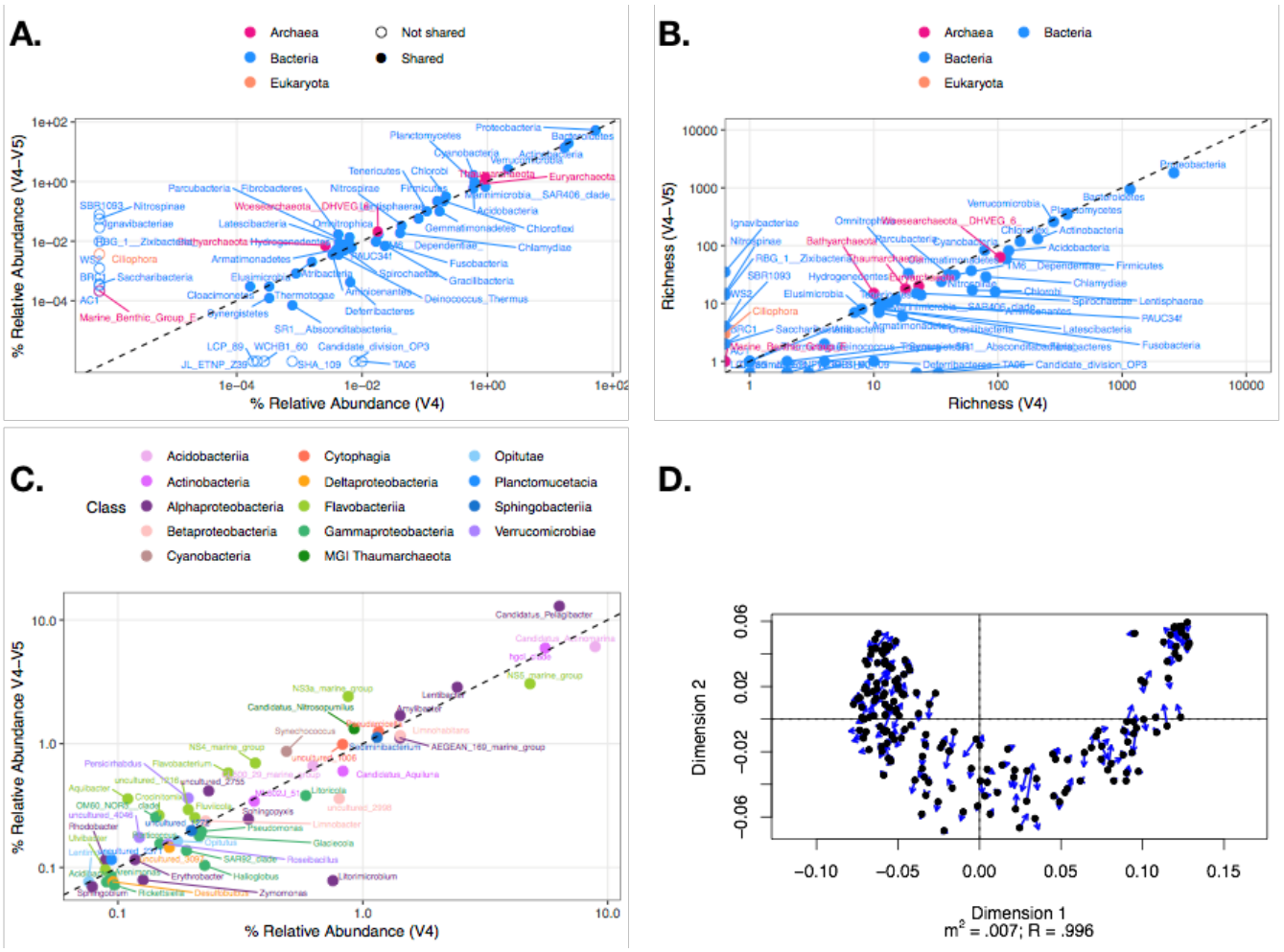

Fig. S3 Comparison of taxonomic and beta diversity between 16S rRNA V4 and V4-V5 primer sets. (A) Comparison between primer sets of relative abundances of phyla. Empty circles indicate phyla found in only one dataset. (B) Of the top 100 genera, the relative abundance of shared genera is shown (excludes “unknown” genera). Point color indicates class. (C) Comparison of richness within each phylum for both primer sets. (D) A procrustes plot of the first 2 axes of PCoA ordinations for both primer sets based on Bray-Curtis dissimilarity. Points indicate sample coordinates for V4 ordination and blue arrows indicate minimized distance to the corresponding V4-V5 ordination coordinates. In A-C the 1:1 line is indicated by the dashed black line.

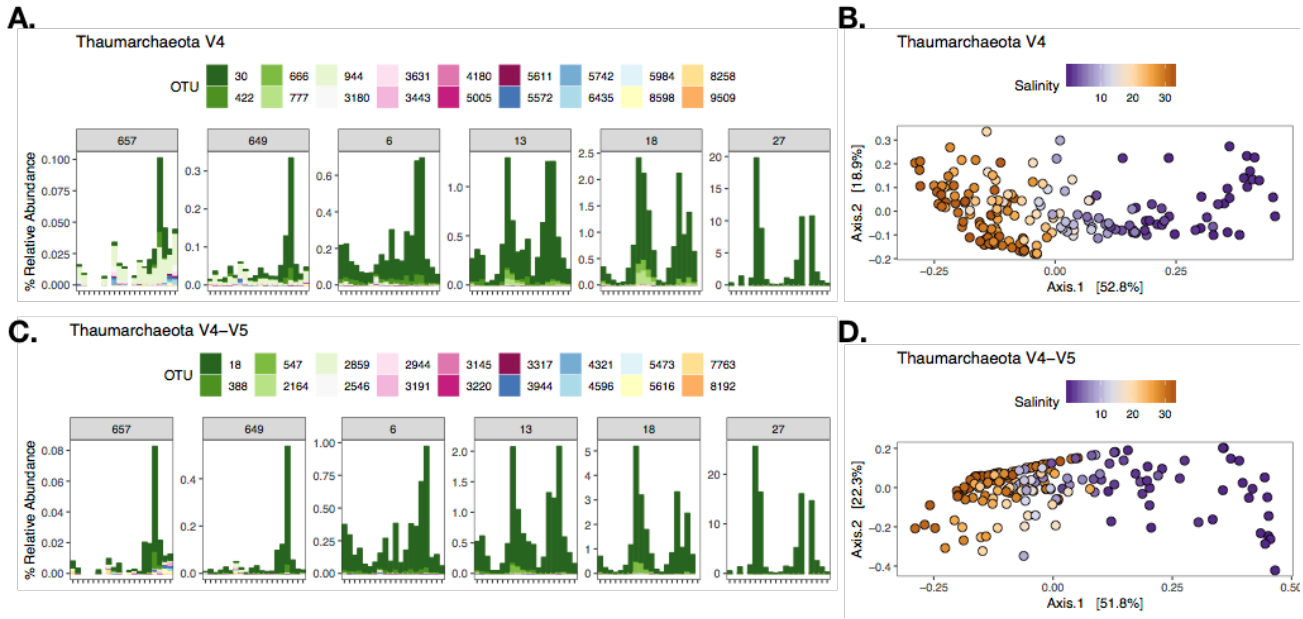

Fig. S4 V4 relative abundance of Thaumarchaeota (A) and beta diversity shown by PCoA based on Bray-Curtis dissimilarity (B) and V4-V5 relative abundance of Thaumarchaeota (C) and beta diversity shown by PCoA based on Bray-Curtis dissimilarity (D). For (A) and (C), panels correspond to 6 representative stations for the five salinity zones and South Bay. The x-axis of each panel corresponds to date of 20 approximately monthly cruises from April 2012 to March 2014. The y-axis is the % relative abundance. Note difference in scale on y-axis between each panel. In (B) and (D), point color corresponds to environmental variable with strongest correlation to axis 1.

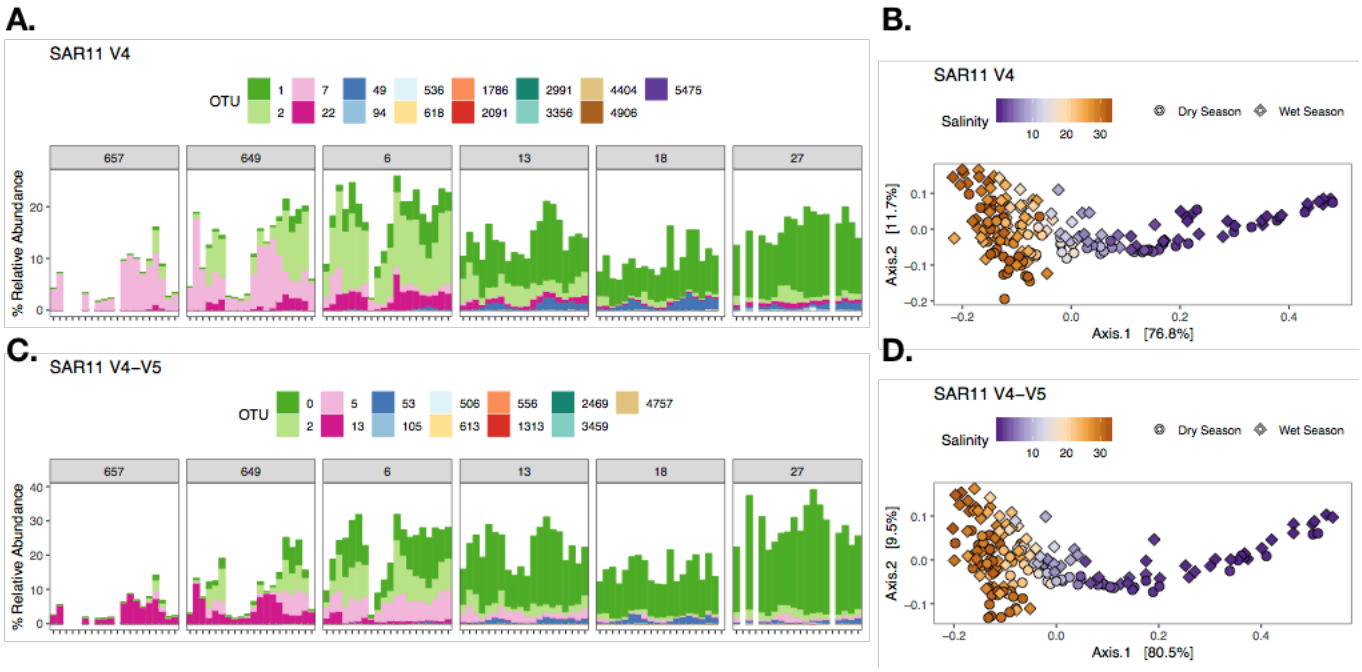

Fig. S5 V4 relative abundance of SAR11 (A) and beta diversity shown by PCoA based on Bray-Curtis dissimilarity (B) and V4-V5 relative abundance (C) and beta diversity shown by PCoA based on Bray-Curtis dissimilarity (D). For (A) and (C), panels correspond to 6 representative stations for the five salinity zones and South Bay. The x-axis of each panel corresponds to date of 20 approximately monthly cruises from April 2012 to March 2014. The y-axis is the % relative abundance. In (B) and (D), point color corresponds to environmental variable with strongest correlation to axis 1 and point shape highlights separation of wet versus dry season samples.

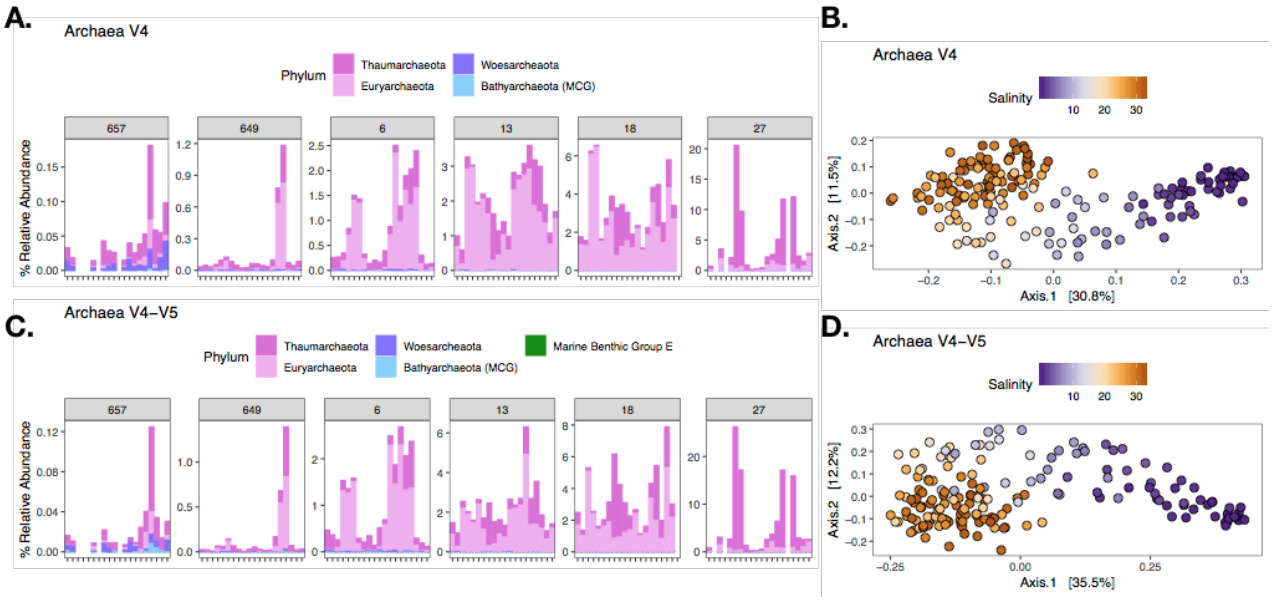

Fig. S6 V4 relative abundance of Archaea (A) and beta diversity shown by PCoA based on Bray-Curtis dissimilarity (B) and V4-V5 relative abundance (C) and beta diversity shown by PCoA based on Bray-Curtis dissimilarity (D). For (A) and (C), panels correspond to 6 representative stations for the five salinity zones and South Bay. The x-axis of each panel corresponds to date of 20 approximately monthly cruises from April 2012 to March 2014. The y-axis is the % relative abundance. In (B) and (D), point color corresponds to environmental variable with strongest correlation to axis 1 and point shape highlights separation of wet versus dry season samples.

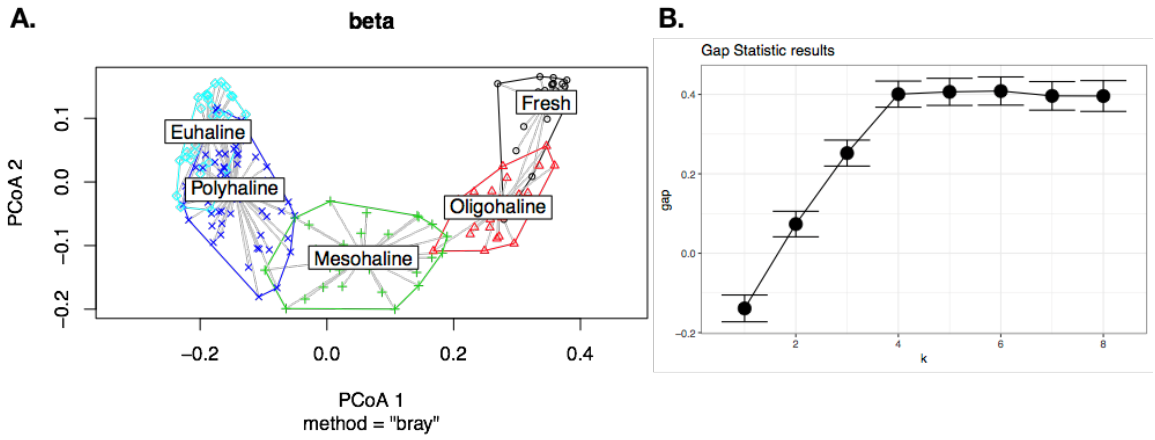

Fig. S7 (A) PCoA ordination with Adonis test of difference between centroids for each salinity zone and (B) gap statistic for goodness of clusters for V4 PCoA ordination based on Bray-Curtis dissimilarity.

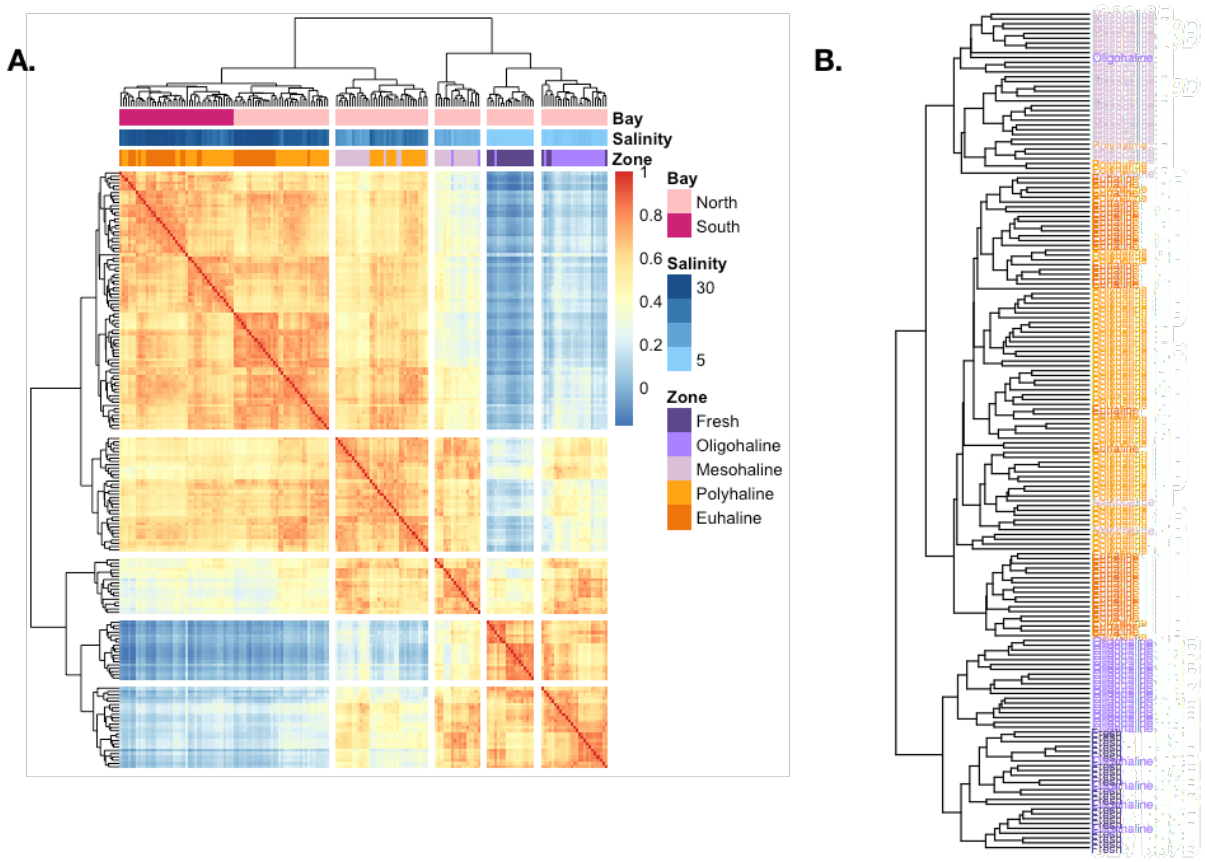

Fig. S8 (A) Heatmap based on Bray Curtis dissimilarity between samples and (B) hierarchical clustering based on Jaccard distance. In (B) tip labels are colored by salinity zone according to the legend in (A).

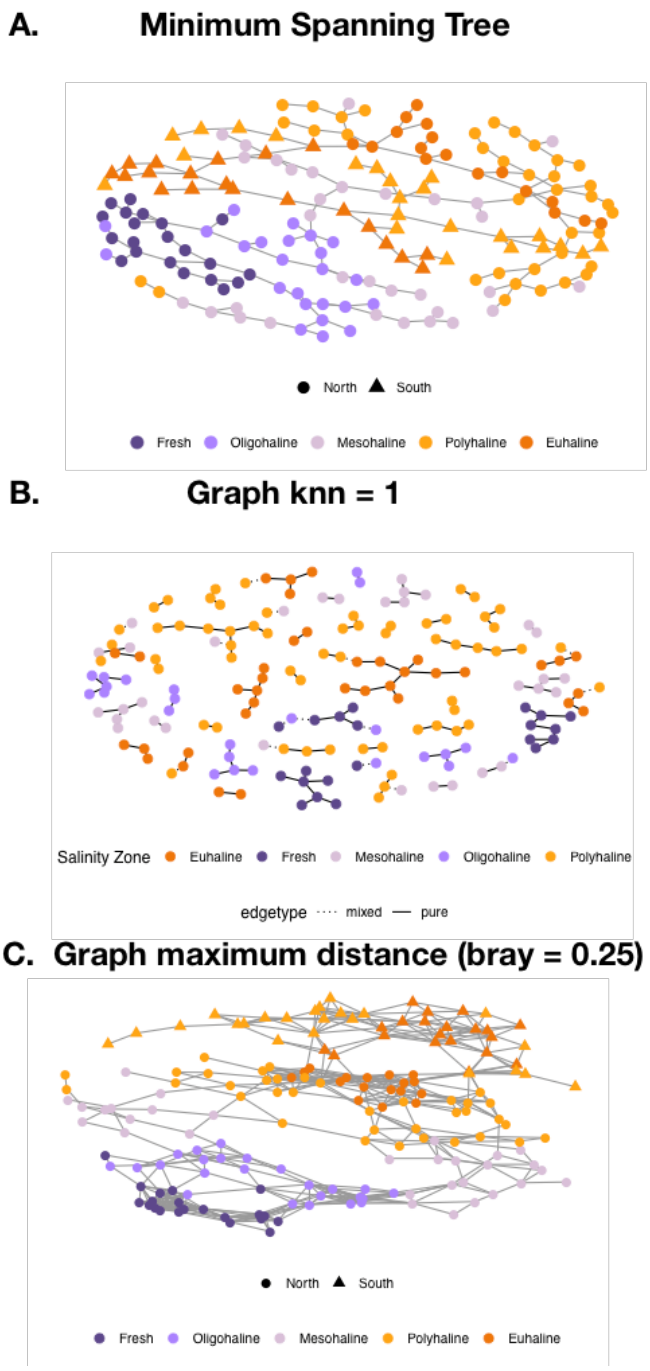

Fig. S9 Graph based on (A) a minimum spanning tree, which connects all samples and minimizes edge lengths based on Bray-Curtis dissimilarity. (B) Graph based on distance-based threshold, making connections between samples with a Bray-Curtis dissimilarity less than 0.25. Solid lines indicate pure edges (samples are in the same salinity zone) and dashed lines indicate mixed edges (connection is between samples of neighboring salinity zone). (C) Graph based on a knn =1, makes connections between nearest neighbor. Solid lines indicate pure edges (samples are in the same salinity zone) and dashed lines indicate mixed edges (connection is between samples of neighboring salinity zone).

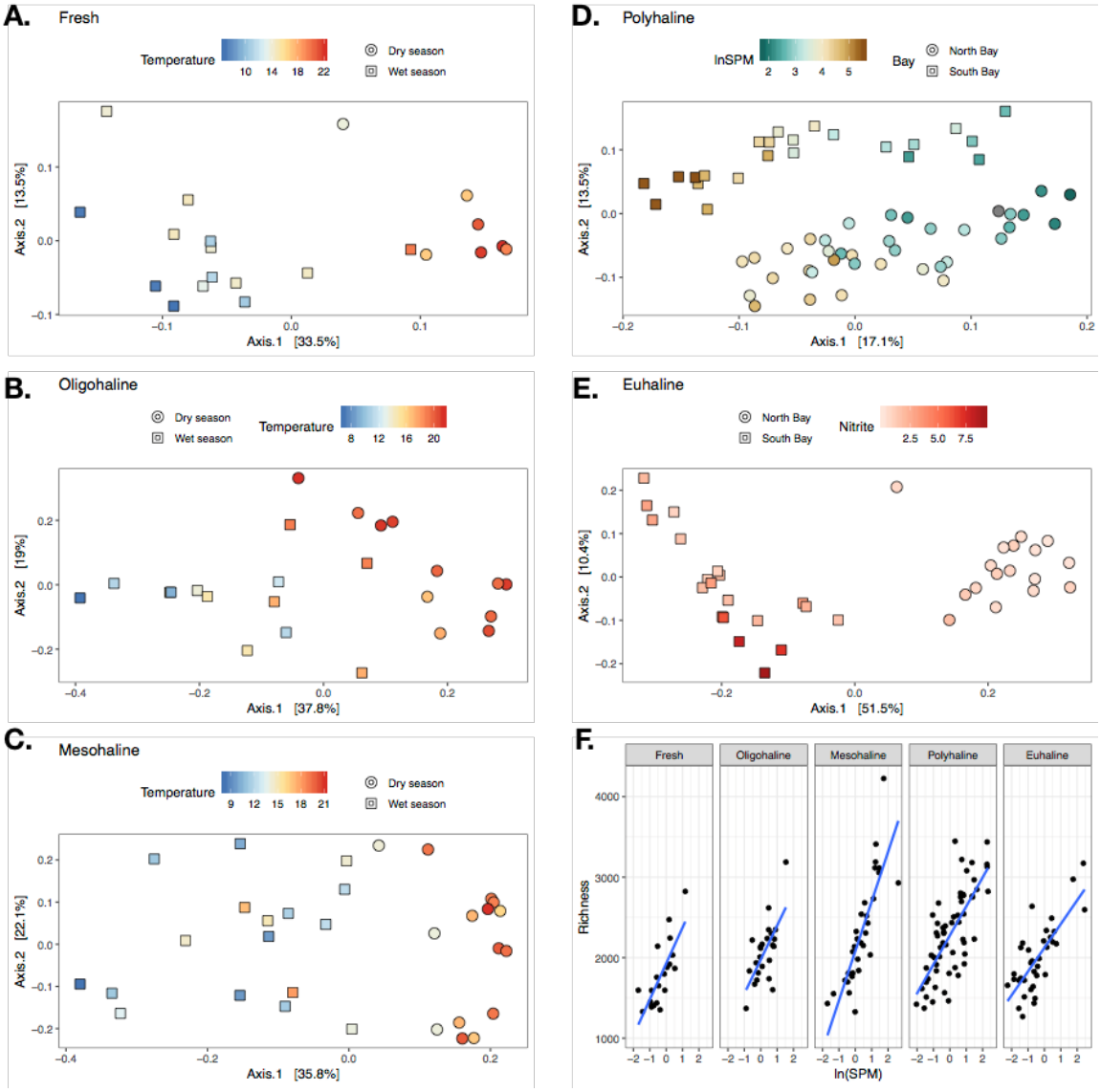

Fig. S10 (A-E) PCoA ordinations based on Bray-Curtis dissimilarity for each salinity zone. Points are colored by strongest environmental correlate with axis 1. Point shape in corresponds to season in (A-C) and bay in (D-E). (F) Shows correlation between SPM concentration and richness within each salinity zone.

Fig. S11 Relative abundance of the most abundant 10 phyla (A), 12 classes (B), 15 orders (C), 18 families (D), and top 24 genera (E). Panels correspond to 6 representative stations for the five salinity zones and South Bay. The x-axis of each panel corresponds to date of 20 approximately monthly cruises from April 2012 to March 2014. The y-axis is the % relative abundance.

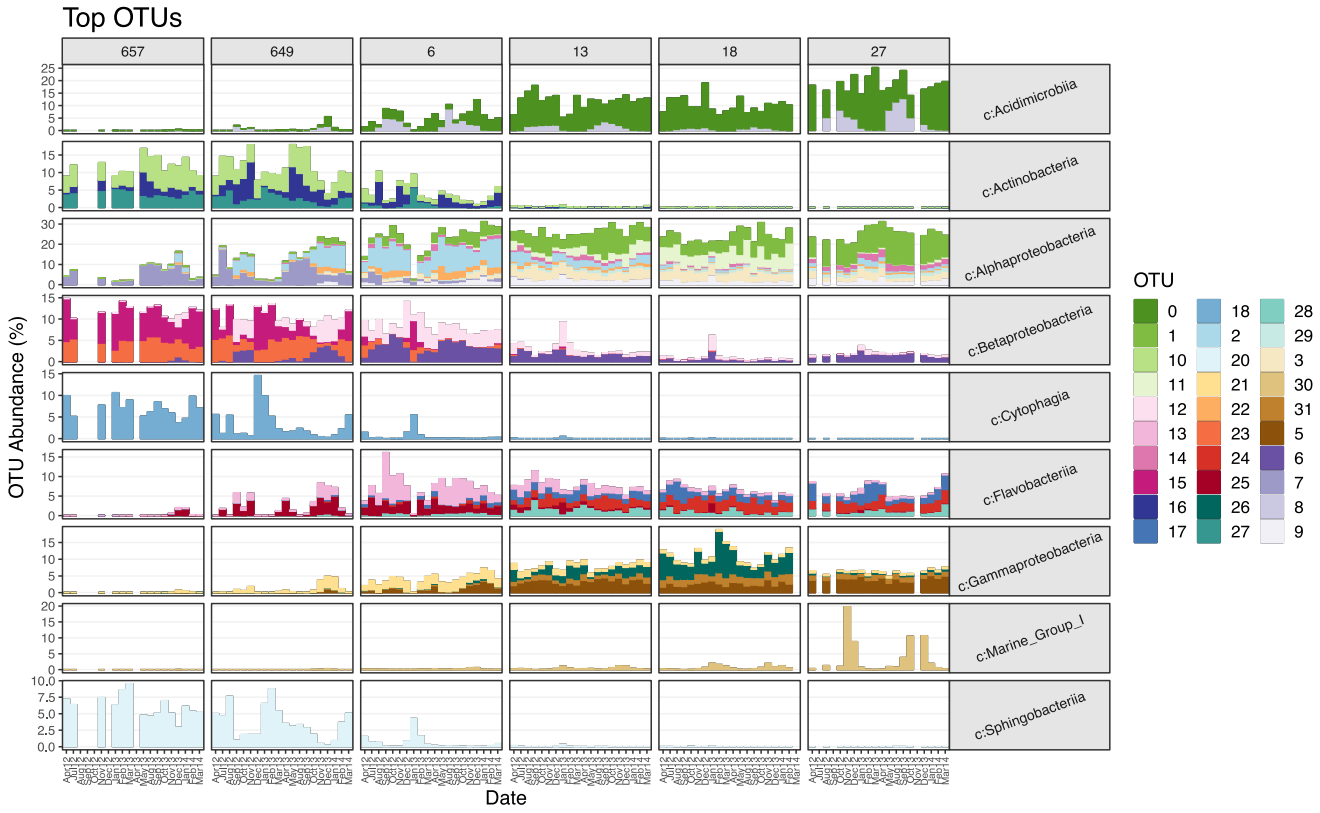

Fig. S12 Relative abundance of the 40 most abundant OTUs in SFB. Panels correspond to 6 representative stations for the five salinity zones and South Bay. The x-axis of each panel corresponds to date of 20 approximately monthly cruises from April 2012 to March 2014. The y-axis is the % relative abundance.

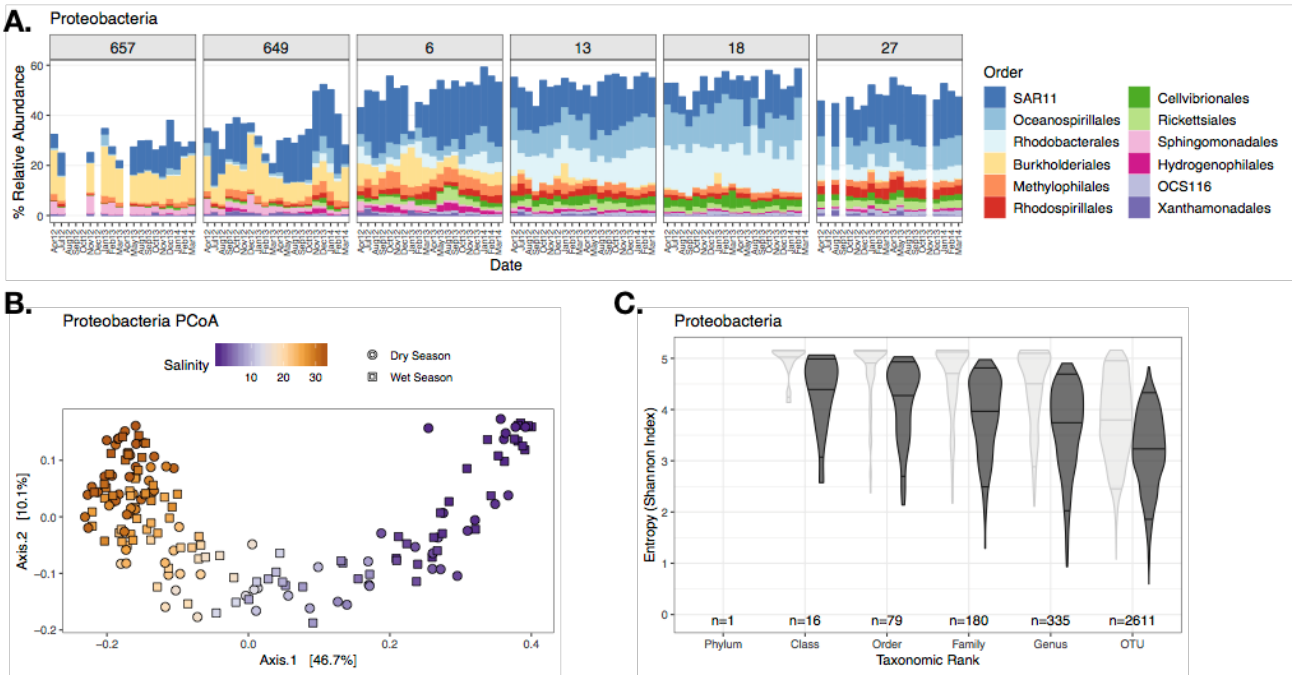

Fig. S13 Proteobacteria diversity metrics. Relative abundance of (A) 10 most abundant Proteobacteria orders. Panels correspond to 6 representative stations for the five salinity zones and South Bay. The x-axis of each panel corresponds to date of 20 approximately monthly cruises from April 2012 to March 2014. The y-axis is the % relative abundance. (B) PCoA ordination based on bray-curtis dissimilarity shows beta diversity is heavily influenced by salinity. (C) Entropy of taxa decreases at finer taxonomic levels, indicating high site-specificity of OTUs.

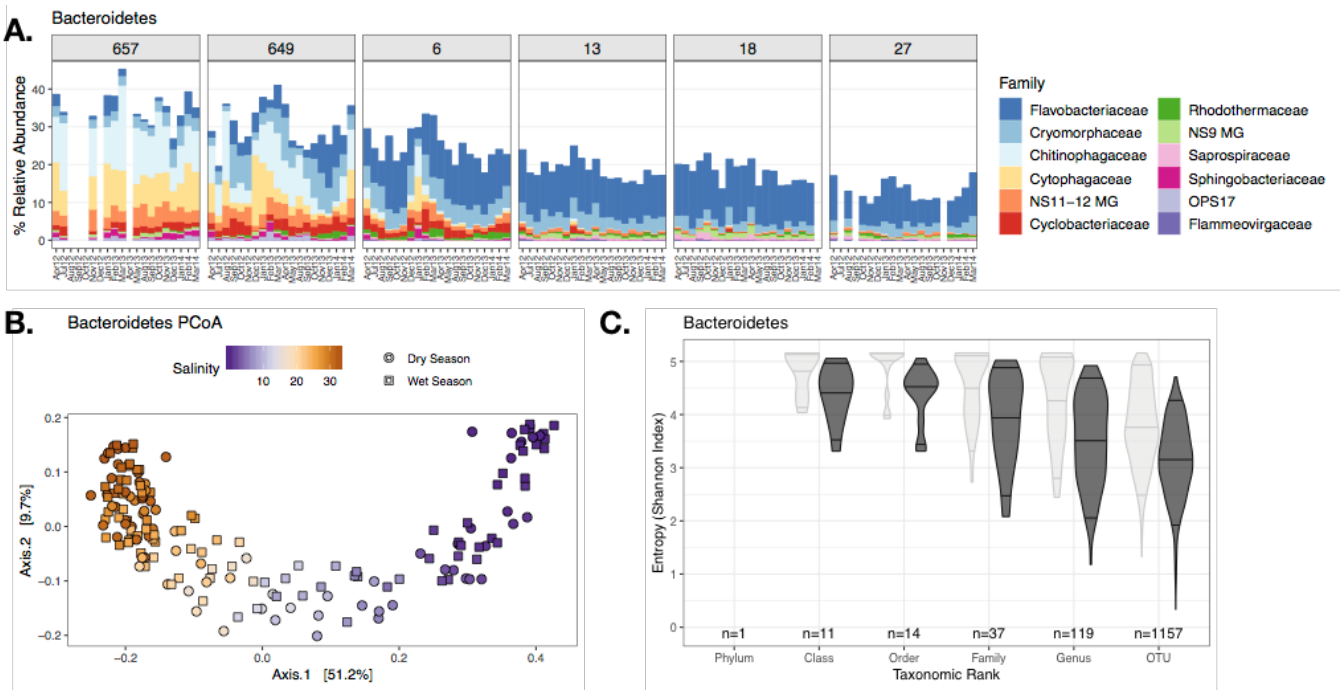

Fig. S14 Bacteroidetes diversity metrics. Relative abundance of (A) 10 most abundant Bacteroidetes families. Panels correspond to 6 representative stations for the five salinity zones and South Bay. The x-axis of each panel corresponds to date of 20 approximately monthly cruises from April 2012 to March 2014. The y-axis is the % relative abundance. (B) PCoA ordination based on bray-curtis dissimilarity shows beta diversity is heavily influenced by salinity. (C) Entropy of taxa decreases at finer taxonomic levels, indicating high site-specificity of OTUs.

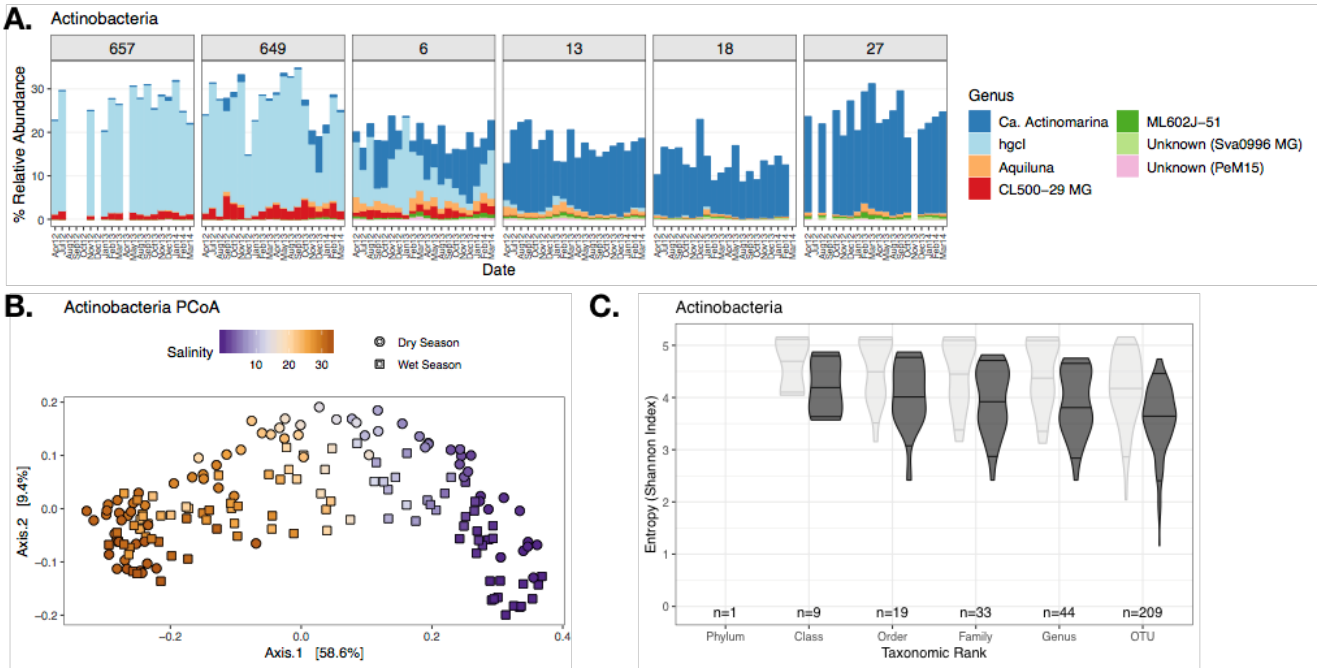

Fig. S15 Actinobacteria diversity metrics Relative abundance of (A) 10 most abundant Bacteroidetes families. Panels correspond to 6 representative stations for the five salinity zones and South Bay. The x-axis of each panel corresponds to date of 20 approximately monthly cruises from April 2012 to March 2014. The y-axis is the % relative abundance. (B) PCoA ordination based on bray-curtis dissimilarity shows beta diversity is heavily influenced by salinity and season (wet versus dry). (C) Entropy of taxa decreases at finer taxonomic levels, indicating high site-specificity of OTUs.

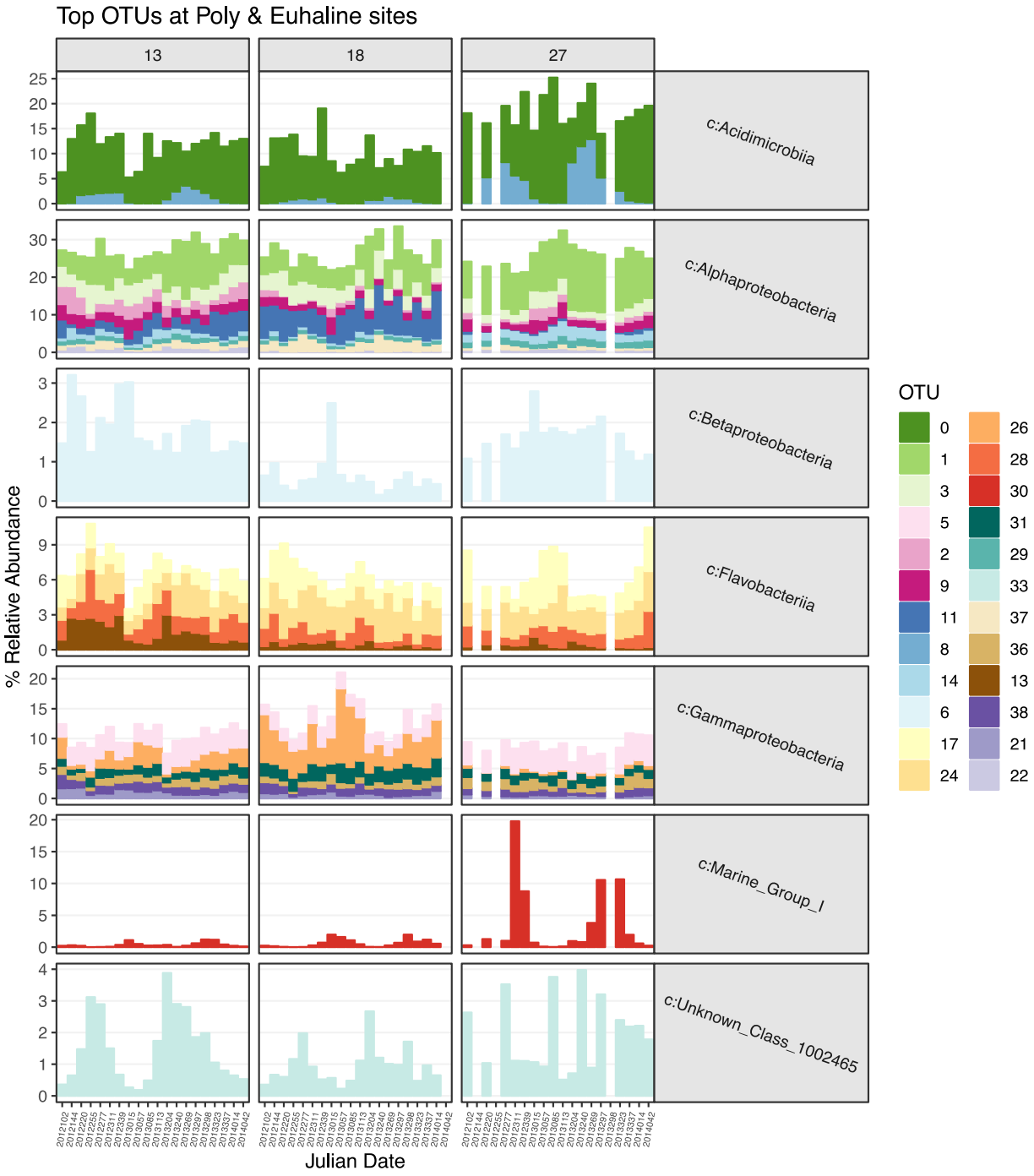

Fig. S16 OTUs in poly and euhaline sites. Panels correspond to 3 generally poly- and euhaline stations, 13 in North Bay, 18 at the mouth of the Golden Gate Bridge, and 27 in South Bay. The x-axis of each panel corresponds to date of 20 approximately monthly cruises from April 2012 to March 2014. The y-axis is the % relative abundance of OTUs.

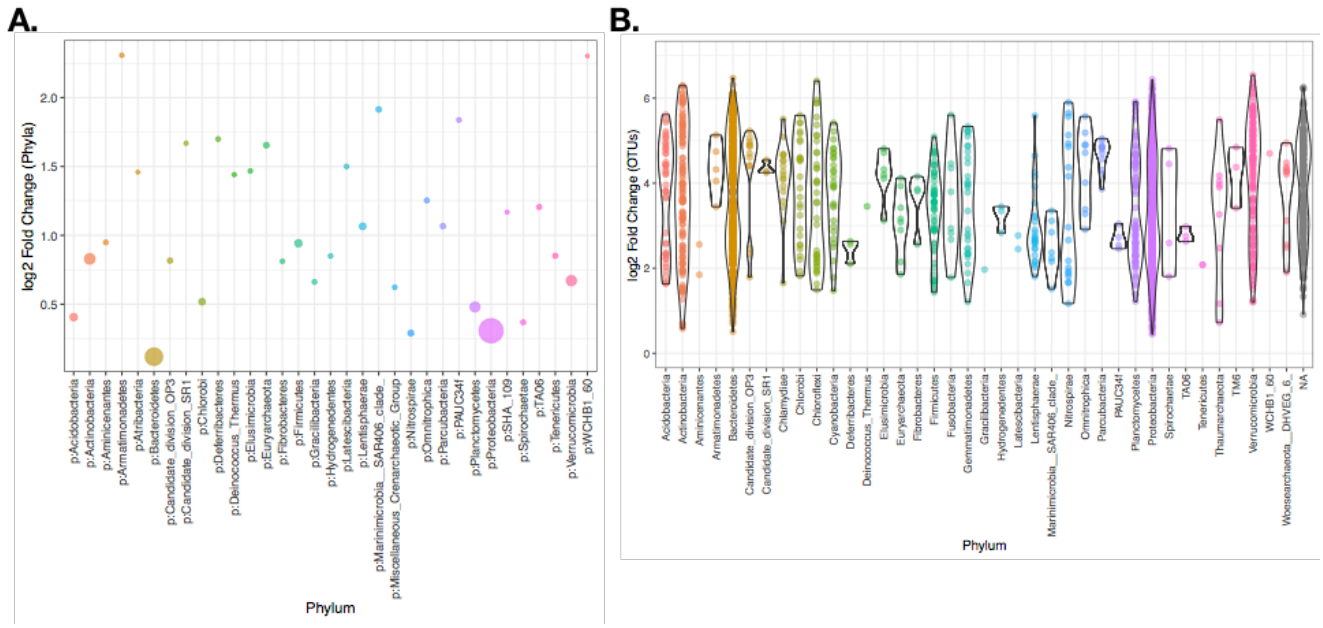

Fig. S17 Differential abundance plots show the log2 fold change of a taxa across salinity zones. Size of points is based on the mean abundance of the taxa.

Fig. S18 Cyanobacteria diversity metrics. Relative abundance of (A) the two most abundant genera (*Synechococcus* and an Unknown *Sericytochromatia*) and (B) PCoA ordination showing beta diversity is most strongly influenced by salinity on axis 1 and season on axis 2. Cyanobacteria show strong summer peaks in abundance and are dominated by *Synechococcus*. Panels correspond to 6 representative stations for the five salinity zones and South Bay. The x-axis of each panel corresponds to date of 20 approximately monthly cruises from April 2012 to March 2014. The y-axis is the % relative abundance. Note the difference in y-axis scale in each row of panels.

Table S1 Taxonomic and read count data for libraries processed through the itagger method and after various filtering stages. Data includes two combined 16S rRNA amplicon (iTag) plates for each primer set.

	V4		*V4-V5*	
	Raw	**>15 reads in >2 samples**	**Raw**	**>15 reads in >2 samples**
Phyla	54	46	63	50
Class	143	123	169	124
Order	292	227	293	207
Family	549	400	510	342
Genera	1064	718	951	610
OTUs	21703	7006	15097	4913
Reads	155,573,985	154,724,570	107,986,733	107,350,210

Table S2 Correlations between environmental variables and diversity metrics for V4 and V4-V5 datasets with the highest and most significant coefficients or of most interest. Referring to PCoAs that include all samples.

		V4		*V4-V5*	
Linear Regression test		***r***	***r²***	***r***	***r²***
OTU					
	PCoA Axis 1 ~ Salinity	-0.97**	0.94	-0.97**	0.94
	PCoA Axis 2 ~ ln(SPM)	0.60**	0.36	0.57**	0.32
	Richness ~ ln(SPM)	0.74**	0.55	0.70**	0.49
	Richness ~ chla/(chla+phaeo)	-0.59**	0.35	-0.52**	0.27
	Richness ~ Salinity	0.056	0.003	-0.11	0.012
Genera					
	Richness ~ ln(SPM)	0.59**	0.35		
	Richness ~ chla/(chla+phaeo)	-0.53**	0.28		
	Richness ~ Salinity	-0.24*	0.06		
Phyla					
	Richness ~ ln(SPM)	0.44**	0.19		
	Richness ~ chla/(chla+phaeo)	-0.31**	0.10		
	Richness ~ Salinity	0.40**	0.16		

**p-value < 0.0001

*p-value < 0.001

values without * have p-value > 0.05

Table S3 Nestedness and turnover components of PCoA ordinations based on Jaccard Dissimilarity. Values were calculated using the beta.core and beta.multi functions which compute multiple-site dissimilarities for spatial turnover and nestedness components of beta diversity, and the sum of both values

Ordination	**Turnover fraction**	**Nestedness-resultant fraction**	**Overall beta diversity**
Whole community	0.972	0.007	0.979
North Bay	0.981	0.005	0.986
South Bay	0.915	0.031	0.946
Fresh	0.840	0.050	0.890
Oligohaline	0.881	0.027	0.908
Mesohaline	0.898	0.036	0.934
Polyhaline	0.944	0.018	0.962
Euhaline	0.917	0.023	0.940

Table S4 Strongest correlation coefficients between environmental variables and diversity metrics for samples in North or South bay or various salinity zones.

	r	r^2
North Bay		
OTU Richness ~ ln(SPM)	0.71	0.50
PCoA Axis 1 ~ Salinity	-0.96	0.92
PCoA Axis 2 ~ lnSPM	0.37	0.14
South Bay		
OTU Richness ~ ln(SPM)	0.88	0.77
PCoA Axis 1 ~ ln(SPM)	-0.89	0.79
PCoA Axis 2 ~ Temperature	-0.70	0.49
Fresh		
PCoA Axis 1 ~ Temperature	0.85	0.72
PCoA Axis 2 ~ Salinity	0.73	0.53
Oligohaline		
PCoA Axis 1 ~ Temperature	0.80	0.64
PCoA Axis 2 ~ Salinity	-0.65	0.42
Mesohaline		
PCoA Axis 1 ~ Temperature	0.76	0.58
PCoA Axis 2 ~ Salinity	0.93	0.86
Polyhaline		
PCoA Axis 1 ~ ln (SPM)	-0.86	0.74
PCoA Axis 2 ~ Distance from 36	-0.86	0.74
Euhaline		
PCoA Axis 1 ~ Distance from 36	0.93	0.86
PCoA Axis 2 ~ Nitrite	-0.57	0.32

all $p < 0.0001$